Butea monosperma seed oil loaded ethosomal vesicular carrier and its hydrogel for vaginal candidiasis: QbD based development, in vitro and in vivo evaluation

Akriti Singh
Shoolini University of Biotechnology and Management Sciences, H.P
Shweta Agarwal
L.R Institute of Pharmacy, H.P
Anuradha Sourirajan
Shoolini University of Biotechnology and Management Sciences, H.P
Arun Parashar
Shoolini University of Biotechnology and Management Sciences, H.P
Kamal Dua
University of Technology Sydney
Dinesh Kumar Chellapan
International Medical University (IMU)
Sachin Kumar Singh
Lovely Professional University
Gaurav Gupta
Suresh Gyan Vihar University
Poonam Negi
poonamgarge@gmail.com

Shoolini University of Biotechnology and Management Sciences, H.P

Research Article

Keywords: Vaginal candidiasis, Butea monosperma, ethosomal vesicles, Box-Behnken design, ethanol

Posted Date: March 5th, 2024

DOI: https://doi.org/10.21203/rs.3.rs-3996093/v1

Additional Declarations: No competing interests reported.

Version of Record: A version of this preprint was published at BioNanoScience on August 21st, 2024.
See the published version at https://doi.org/10.1007/s12668-024-01575-x.

Abstract

Purpose

Vaginal candidiasis (VC), a common recurrent gynaecological disorder affects almost 70% women. Development of resistance to antifungal agents exacerbates the need for new treatments against *Candida* infections. The objective of the current work was to develop Ethosomal Vesicles (EVs) and EV hydrogel of Butea monosperma seed oil (BMSO) for treatment of vaginal candidiasis as BMSO has demonstrated fungicidal and bactericidal activity.

Methods

EVs, formulated by ethanol injection-sonication method used Phospholipon90G and ethanol as excipients and were optimized by Box-Behnken design (BBD). BMSO (X_1), phospholipid (X_2) and ethanol concentration (X_3) were selected as input variables, while vesicle size (Y_1), PDI (Y_2) and %EE (Y_3), were taken as response variables.

Results

The size of optimized EVs was found to be 240.9nm, PDI was 0.326, %EE was 53.84%. FESEM and HR-TEM unveiled vesicles of rhombic dodecahedral shape with smooth, sealed structure. The EVs, incorporated into carbopol gel demonstrated non-Newtonian behavior. *MIC* determination by broth microdilution method revealed MIC of EVs and hydrogel to be 2.5 times less as compared to BMSO against *C. albicans*. Anti-*candidal* activities determined using agar well diffusion method demonstrated better zone of inhibition for hydrogel vis-à-vis BMSO. Pharmacodynamic evaluation manifested comparable decrease in fungal burden by EVs and EV hydrogel to marketed Clotrimazole. Histopathology of vaginal tissue of treated groups showed no or mild inflammation with normal skin structure.

Conclusion

The results disclosed EVs and EV hydrogel to possess better antifungal activity vis-a-vis BMSO and can be explored as potential alternative herbal product for VC.

1. Introduction

Vaginitis also known as vulvovaginal candidiasis (VVC) or vaginal candidiasis (VC) is a common gynaecological disorder which recurrently occurs when estrogen levels surge, especially during pregnancy. The most common yeast isolated from this condition is *Candida albicans* (*C. albicans*) (85–

90%). The rising incidence of vaginitis could be due to different reasons viz., excessive use of antifungal agents, single dose treatments, low dosage azole maintenance regimens or increased number of high-risk patients (e.g. diabetics and HIV women) etc (Srivastava et al., 2018). *Candida* infections are mainly superficial, but in severely immunocompromised patients systemic infections can occur. Most, if not all women carry *Candida* in vagina at some point of their lives, yet without symptoms of infection. *Candida* organisms gain access to the lower genital tract mainly from the adjacent perianal area. VVC is not a reportable disease, and therefore, the information on its incidence is incomplete and based on epidemiology studies that are often hampered by inaccuracies of diagnosis and/or the use of non-representative populations. VVC is considered the second most common cause of vaginitis after bacterial vaginosis (BV) (Goncalves et al., 2015).

Vast varieties of plants harbor extraordinary potential in treatment of various ailments and infectious diseases. *Butea monosperma (*BM) (Lam.) Taub is one such example, commonly known is 'Flame of forest' and Bastard Teak. It is a medium- sized tree belonging to family Fabaceae. It is considered as a good source of gum, resin, food, fibre, dye and traditionally being used for the treatment of number of diseases such as cancer, diabetes diarrhoea and dysentery (Sutariya and Saraf, 2015). It also works as an appetizer, laxative, anthelmintic and aphrodisiac etc. The extracts of following parts of plants such as flower, gum, seed, leaf, and bark have been employed in various studies. The various parts of BM contains many active constituents e.g. butein, butrin, flavonoid and steroids (flower), glucose, glycosides (roots) tannin (gum), oil, proteinase and polypeptidase (seed) etc (Tiwari et al., 2019).

Though these active constituents have shown their activity in manifesting various immunomodulatory effects, anti-tumorogenic activity and modulation of cell signaling, still their full potential stands to be assessed (Chauhan and Mahish, 2020).

Several investigations regarding therapeutic and beneficial effects of extracts of various parts of plants have been carried out. Ethanolic extract of BM flowers exhibited significant reduction in blood glucose, serum cholesterol, improved HDL-cholesterol and increased the activities of antioxidant enzymes. Similarly, methanolic extract of BM flowers showed lipid lowering and anti-diabetic activity against high fat diet and streptozotocin induced diabetes in rats (Sutariya and Saraf, 2015).

The ethanolic and methanolic extracts obtained from BM seeds have been shown to possess antidiabetic, anti-hyperlipidemic and antiperoxidative, antifertility, antiviral effects. The ethanolic extract treated for four weeks exhibit significant antihyperglycemic effect with improved glucose tolerance in non-insulin dependent diabetic (NIDDM) rats (Tiwari et al., 2019). BM seed oil showed a significant fungicidal and bactericidal effect *in vitro* which may be due to the presence of active constituents like medicarpin (Tiwari et al., 2019).

Previously reported research on BM seed oil indicated various pharmacological applications for both internal and external uses. Formulating an ethanolic vesicular hydrogel system will help to extend the retention time, improve the penetration, spreadability and skin adhesion. Additionally, based on our search, novel formulations such as nanoemulsion, microemulsion or liposomes have not been reported

so far for BM seed oil. The present work intends to develop ethosomal vesicles (EVs) and ethosomal vesicular hydrogel of BM seed oil for topical application and evaluate its antifungal activity. (Cupara et al., 2012).

2. Materials and Methods

2.1 Materials

BM seed oil was obtained from Suyash Ayurveda, Gujarat. Lipoid, GmbH provided a complimentary sample of Phospholipon 90G (PL90G) from Germany. Hexane, ethanol, dimethyl sulphoxide (DMSO), triethanolamine (TEA), potassium hydroxide (KOH), sodium hydrogen sulphate ($NaHSO_4$) were purchased from Mumbai-based Loba Chemie Pvt. Ltd. India. Sodium sulphate anhydrous was procured from Thomas Baker Pvt. Ltd. Mumbai, India. Carbopol 934, Yeast Extract-Peptone-Dextrose, Roswell Park Memorial Institute- 1640 medium, Mueller Hinton Broth, Mueller Hinton Agar media were procured from Himedia Laboratories, Pvt, Ltd. Mumbai, India. Formaldehyde solution was procured from CDH Pvt. Ltd., New Delhi, India. Clotrimazole cream, used in the *in vivo* studies, was procured from local pharmacy. Other chemicals were of analytical grading, and glasswares were borosilicate.

2.2 Methods

2.2.1 Analysis of BM seed oil by Gas Chromatography (GC)

Derivatization of fatty acids present in BM seed oil

The fatty acids in seed oil of BM (20 µL) were transformed to fatty acid methyl esters (FAME) for evaluation using gas chromatography/mass spectroscopy. Fatty acids in 20 µL of oil were transesterified at 55°C for 1.5 hours in 0.7 mL of 10 N KOH, and 5.3 mL of methanol in a water bath. This was allowed to cool before adding 0.58 ml of 24 N H_2SO_4 and reversing the process. After another 1.5 hours of incubation at 55°C, the sample was cooled down. 3ml hexane was added and then vortexed for 5 minutes followed by centrifugation at 5000 rpm for 5 minutes. The esterified compound obtained in the hexane layer was further tested by GC for estimation of alkyl derivatives that is methyl esters formation of fatty acids (FAME) (Ito et al., 2014; European Pharmacopeia, 5th ed).

Chromatographic system

On the gas chromatograph (GC-2014), a flame ionization detector and a 0.25 mm 30 m fused silica capillary column encapsulated with a 0.25 µm FAMEWAX™ column (cat # 12497) were installed (GC-2014). The injection port and detector temperatures were kept at 225°C and 230°C, respectively. The column temperature process was initially set to 165°C for the first 30 minutes, then increased at a rate of 1.5°c/min to 220°C, where it remained stable for the final 15 minutes. The carrier gas, helium, was partitioned with a flow ratio of 1:40 at an initial temperature of 40 cm/sec and a flow rate of about 0.5 mL/min.

2.2.2 Physical characterization of oils

BM seed oil was evaluated for physical characteristics which included color, odor and clarity.

2.2.3 Development of BM seed oil-loaded EVs

In the present research work, EVs were formulated using BM seed oil for treating VVC using the ethanol injection-sonication method.

BM seed oil and PL90G were dissolved in ethanol (organic phase) and then the organic phase was firmly injected dropwise into the aqueous phase with a syringe for half an hour with constant stirring at 1000 rpm and sonicated for 20 minutes. The prepared BM oil loaded EVs were refrigerated for further characterization and evaluation. The preparation process is exhibited in the Fig. 1.

2.2.4 Selection of Phospholipid

The ability of various phospholipids to form ethanolic vesicles (EVs) with desired properties was tested. PL 90G, Phospholipon 85G (PL 85G), and liquid lecithin were among the phospholipids studied. Phospholipids were used without further purification.

2.2.5. Selection of concentration of BM seed oil, ethanol, and phospholipid

A total of 6 formulations were synthesized with BM seed oil, ethanol and phospholipid ranging in concentration from 5–15%w/w, 10–25%w/w, and 5–10% w/w respectively during preliminary studies (Touitou et al. 2000), displayed in Table 1.

Table 1
BM seed oil, phospholipid and ethanol concentrations in various preliminary EV formulations

Formulations	BM seed oil (g) (F1-F6)	Ethanol (g)	PL 90G (g)
F1	0.5	1	1
F2	0.5	2	1
F3	0.5	2.5	1
F4	1.5	1	1
F5	1.5	2	1
F6	1.5	2.5	1

2.2.6 In-process Vesicle Monitoring

Throughout the studies, prepared EVs were monitored for structural integrity and micromeritics using a high accuracy optical microscope (magnification: 40X, 100X) equipped with a camera. During the

studies, various vesicular properties such as shape, vesicle count, percent light transmittance, disruption, lamellarity, vesicle coalescence, aggregation, and physical stability of the drug for 15 days in the vesicles were supervised.

2.2.7 Systematic optimization of BM seed oil loaded EVs as per the experimental design

QbD is a systematic, organised process concerned with pharmaceutical product quality. It then runs specific key factors representing the independent variables and examines their impact on the dependent observed responses. In other words, QbD provides and implements a composition — for the model to be designed and meet the specified standards. Response surface methodology (RSM) is a tool that generates a large amount of data with minimal input. (Ismail et al., 2021).

A 3-factor, 3-level BBD was used to optimise BM seed oil-loaded EVs (BBD). The chosen dependent variables were the concentration of BM seed oil (X_1), PL 90G (X_2), and ethanol (X_3), applied at 3 distinct levels of each variable, *viz*. low (5%), medium (17.5%), and high (25%). The response variables *viz.* vesicle size, PDI and entrapment efficiency (%EE) were evaluated using numerous ethanolic vesicular formulations prepared according to the design. Table 2 outlines the 17 experimental runs analysed, as well as the coded values for the studied factors. Following the evaluation of prepared EVs for the response variables, optimization statistics analysis was accomplished. Design Expert® ver.10.0.1 was used to produce 3-D response surface plots and 2-D contour plots for the response surface evaluation (MS Stat-Ease Inc., Minnepolis, MN) (Negi et al., 2015).

Table 2
Factor combinations as per the chosen experimental design (i.e., BBD) for BM seed oil-loaded EVs

Codes of EVs	Trial No.	Coded Factor levels		
		X_1	X_2	X_3
F1	1	-1	0	1
F2	2	-1	0	-1
F3	3	1	0	-1
F4	4	-1	-1	0
F5	5	0	0	0
F6	6	0	1	-1
F7	7	0	0	0
F8	8	0	0	0
F9	9	0	-1	1
F10	10	0	0	0
F11	11	0	0	0
F12	12	1	-1	0
F13	13	1	0	1
F14	14	-1	1	0
F15	15	1	1	0
F16	16	0	-1	-1
F17	17	0	1	1
Actual unit translation of coded levels				
(BM-EVs)				
Coded level (EV1 to ETHO17)		**-1**	**0**	**1**
X_1: BM seed oil (%)		5	10	15
X_2: PL (%)		5	7.5	10
X_3: Ethanol (%)		10	17.5	25

2.2.8 Characterization of prepared EVs

Particle size of BM seed oil loaded EVs

Particle size and ethanol concentrations have an impact on skin permeability and are considered as vital parameters. The small vesicle size allows for good penetration through the skin. Zetasizer from Malvern, UK was used to assess the average diameter and PDI of the prepared BM seed oil-loaded EVs (Malvern, UK). The samples (1ml) were analysed 24 hours after they were prepared. The samples were inserted in a polystyrene sample cell, and the results were kept track of. To circumvent multi-scattering phenomena, EV dispersions were diluted 1/4th with distilled water prior to measuring of particle size, and each sample test was performed three times. A photomultiplier was used to quantify the intensity of the laser light dispersed by the samples at a 90º angle. Because of random collisions with solvent molecules, particles suspended in fluids were in Brownian motion. The diffusion coefficient is inversely proportional to particle size, according to the Stokes-Einstein equation. The width of the size distribution was measured using PDI. A PDI of less than 0.4 indicates that the vesicles are homogeneous and monodisperse (Pathan et al., 2016).

High resolution Transmission Electron Microscopy (HR-TEM) BM seed oil-loaded EVs

The samples' surface morphology was evaluated using HR-TEM. A drop of prepared EVs was put on a carbon film-covered copper grid prior to the observation, and the specimen was negatively stained with a single drop of 1% aqueous sodium phosphotungstate solution. After removing excess liquid, the specimen was allowed to air dry prior to TEM evaluation (Safwat et al., 2017).

Field emission scanning electron microscope (FESEM) of the BM seed oil-loaded EVs

FESEM also assessed the shape and size of the EVs. On a clear glass stub, a single drop of EVs was mounted. They were then air-dried and encapsulated with a very thin gold coating to allow for FESEM visualisation.

FESEM has been developed as a modern version of SEM with a magnification of approximately 300,000x and an increasing voltage range of about 0.1 to 30 kV is used. Despite having the same instrument configuration, FESEM is preferred over SEM due to higher image resolution. The cold cathode field emitter of a field emission gun (FEG) heats up the tungsten filament by immersing it in a large power potential gradient, which distinguishes the FESEM from the SEM. The electric gun creates a strong vacuum in the cabinet, outperforming the traditional tungsten filament and enabling for faster scanning than SEM. Furthermore, using metal apertures and magnetic lenses, electron beams in FESEM are constrained and concentrated into a thin monochromatic beam (Mahmood et al., 2017).

Percent entrapment efficiency (%EE)

The GC FAME method was used to calculate the %EE of BM oil-loaded EV. Using the centrifugation method, the % EE was measured in triplicate. The EVs were centrifuged at 10000 rpm (M/s REMI CPR 24) for 10 minutes at 4^{o} C. After lysing with hexane, the drug content was identified in both the vesicular sediment and clear supernatant.

The following equation was used to calculate the drug's % EE:

$$\%EE = \frac{T-C}{T} \times 100$$

where, T denotes the total amount of drug found in both the sediment and the filtrates, and C denotes the amount of drug found only in the supernatant (Negi et al., 2017).

2.2.9 Preparation of ethanolic vesicular hydrogel

Carbopol 934 tends to form a very good consistency and clear gel at low concentrations. A small amount of distilled water was used to soak Carbopol 934 for an hour. Triethanolamine was then used to adjust the pH to neutral. Under continuous stirring, the required amount of BM seed oil-loaded EVs were added to the swollen polymer until homogeneous, clear, and transparent gel was achieved (Shukla et al., 2020; Indora and Kaushik, 2015).

2.2.10 Characterization of ethanolic vesicular hydrogel

Rheological studies

Rheological analysis is a crucial component of quality control. Rheological parameters such as yield point, flow behaviour, thixotropy, and apparent viscosity can all help predict how a product will react during preparatory work, handling, and finally skin application. Rheological measurements were conducted within 24 hours of preparation (Wojciechowska et al., 2021).

Rheological studies on the optimised ethanolic vesicular hydrogel were carried out using a rotary type rheometer (Rheolab QC, M/s Anton-Paar GmbH, Vienna, Austria) equipped with DG26 spindle geometry for assessing the sample's viscosity and torque and a water jacket (C-LTD80/QC) to keep a constant temperature of 25°c. The optimised formulation was subjected to individual shear rate and shear stress conditions, and data were analysed using Rheoplus/32 ver 3.40. Shear stress was gradually increased from 0.1 to 100 s^{-1}. For all samples evaluated in triplicate, the mean value was calculated using the Power-law and Herschel-Bulkey models (Garg et al., 2017).

2.2.11 Minimum Inhibitory Concentration (MIC) determination of BM seed oil loaded EVs and ethanolic vesicular hydrogel in fungal strains

Fungal strain of *Candida* (ATCC 90028) was used for this study. At 4°c, the fungal strains were maintained in YPD broth and agar media.

MIC is referred as the extract’s minimum concentration needed to prevent/arrest the development of all microorganisms in the culture (Soumya and Nair, 2012).

Heat maps were designed to assist in the visualisation of antifungal susceptibility data, with optical density values represented quantitatively with colour. In flat-bottom 96-well microtiter plates containing

RPMI 1640, the MIC of BM seed oil-loaded EVs and ethanolic vesicular hydrogel against the test fungus was determined.

The BM seed oil-loaded EVs and ethanolic vesicular hydrogel were selected from the 10% x-axis range. Each well received 50 µl of working inoculum suspension (1×10^8 cfu/ml). A number of wells in each plate were set aside for sterility (no inoculum), inoculum survival (no sample solution), and inhibitory effect control with dimethyl sulfoxide (DMSO) (no sample added). For 48 hours, the plate was incubated at 30°C. The colour change was then visually observed after the dye resazurin was added. Colour change from purple to pink or colourless indicated growth. MIC values were determined by the lowest concentrations at which the colour changed from purple to pink.

2.2.12 Anti*candidal* activity by agar well diffusion

The agar well diffusion assay is commonly used to test the antifungal potential of BM seed oil loaded EVs and ethanolic vesicular hydrogels. Agar well diffusion was carried out with the help of agar extract and yeast extract peptone dextrose broth (YPD). The media was autoclaved for 15–20 minutes at 121° cointegrated at 15psi. Following that, the media was transferred into Petri plates within the laminar airhood and agar was allowed to solidify. After the medium solidified, four 4 mm diameter wells were snipped out of the agar and each well received 10 µl of the antifungal agent (fluconazole, positive control), BM seed oil loaded EVs, ethanolic vesicular hydrogel, and DMSO (negative control). The plates were kept for 42–72 hours at 35ºc. The diameter of a clear zone of inhibition for fungal growth was later determined.

2.2.13 Vaginal candidiasis mice model for in vivo studies

For the current study, pathogen-free BALB/c female mice (20–25 gm) were divided into four groups. The animals were kept in the *in vivo* testing facility at 25 ± 3ºC with a 12-hour light/dark cycle, and were fed a nutritious diet and pure water. The CPCSEA approved all animal experiments and the study through the Institutional Animal Ethics Committee of Shoolini University (Protocol no. IAEC/SU/21/01).

C. albicans was cultured on Sabouraud's dextrose agar. Prior to vaginal *C. albicans* infection, mice were given a single cyclophosphamide dose, intraperitoneally (200 mg/kg body weight). Estradiol valerate in the dose of 0.5 mg/mice was subcutaneously given from day − 3 to day + 4 (8 days) to stimulate the condition of pseudo estrous. For three days, vagina of mice was inoculated with a clean and fresh suspension of *C. albicans* (50 µl) comprising 1.2×10^9 colony forming unit/ml (cfu/ml) (day 0, 1, 2).

Itching, vaginal discharge, redness, and high swelling appeared three days later. The test substances were administered intravaginally to mice (50 mg each of BM seed oil, BM seed oil-loaded EVs, and ethanolic vesicular hydrogel) after infection was confirmed. Infection control was presented by a group that was infected but not treated, while negative control was presented by a group that was neither infected nor treated. The standard group received marketed cream (clotrimazole, 50 mg) once daily for three days (Srivastava et al., 2018).

2.2.14 Histopathological analysis of vaginal tissue

Following the completion of the *in vivo* study, the animal was killed and the medicated skin area was removed. Each sample was fixed in 10% formalin solution before being cut into transverse sections for histological evaluation. Before being examined microscopically for changes in vaginal tissue, samples were properly analysed and stained with haematoxylin-eosin (Kirici et al., 2021).

3. Results and discussion

3.1 GC analysis of derivatized fatty acid BM seed oil

The BM seed oil was found to be completely miscible in methanol and hexane. The miscibility of BM seed oil in the selected solvent was required for the esterification of fatty acids. Methyl ester, derivatized from BM seed oil were further analysed by gas chromatography (GC). Table 3 shows the retention time and area of fatty acids present in seed oil of BM.

Chromatograms of fatty acid present in BM seed oil i.e. oleic acid is shown in Figure no. 2. The results of GC analysis confirmed the presence of oleic acid in the BM seed oil, that was used for formulation and assessment of BM seed oil-loaded EVs and ethanolic vesicular hydrogel. Linoleic acid and oleic acid at 1000 µM completely inhibit the growth of all fungi in liquid culture. Linoleic and oleic acid inhibit *Pyrenophora avenae* growth by 72% as reported by Walters et al. (Walters et al., 2004).

Table 3
GC of BM seed oil

S. No.	Retention time	Area (%)	Name
1.	20.82	7.31	Oleic acid

3.2 Physical attributes of BM seed oil

BM seed oil was subjected to physical characterization for its colour, odour and clarity as shown in Table 4.

Table 4
Physical attributes of BM seed oil

S.No.	Features of BM seed oil	Observations
1.	Color	Dark orange
2.	Odor	NIL
3.	Clarity	Clear and transparent

3. 3 BM seed oil-loaded ethanolic vesicles (EVs)

3.3.1 Selecting Phospholipid (PL) Types

Phospholipon 90G (PL 90G) was chosen from a large pool of PLs due to its appropriateness for EVs as can be seen from Table 5. In ethanol, phospholipon 90H (PL90H) was not readily dissolvable. The EVs prepared using PL90G showed no detachment of the drug with very little accumulation (Table 5), so it was chosen for synthesizing EVs.

Table 5
Formulation characteristics of various batches of EVs for selection of PL

PL	Turbidity	Degree of Accumulation	Shape	Separation of drug	Size
Lipoid S-100	Less	High	Spherical	Yes	Small
PL85G	Moderate	Medium	Spherical	Yes	Small
PL90NG	Moderate	Medium	Spherical	No	Small
PL90G	High	Low	Spherical	No	Small

3.3.2 Selection of BM seed oil, ethanol and PL concentrations

Table 6 shows the vesicular characteristics, such as turbidity and degree of accumulation, of samples made with various concentrations ranges of ethanol and PL90G. It was discovered that PL90G and ethanol modified the EVs' various vesicular properties (Ascenso et al. 2015). Ethanol can engage with the hydrophilic head of lipid molecules, significantly reducing the melting point of subcutaneous lipids and increasing fluidity and cell membrane penetrability. Furthermore, high ethanol concentration will alter the surface properties of the vesicles, decreasing particle size. As a result, large amounts of ethanol are used for the development of small ethosomes (Limsuwan and Amnuaikit, 2012). Out of a total of 6 combinations, formulations F3, F6, formed a clear solution with no visible vesicles. As a result, for optimization studies, the concentration variations of BM seed oil, ethanol, and PL were chosen to be 5–10%, 10–25%, and 5–10%, respectively.

Table 6
Formulation attributes of various BM seed oil-loaded EVs batches for selection of PL and ethanol concentration

Formulations	Seed oil	Turbidity	Degree of accumulation
BM			
F1	0.5	#####	High
F2	0.5	###	Medium
F3	0.5	Clear solution	_____
F4	1.5	####	High
F5	1.5	#	Low
F6	1.5	Clear solution	_____

3.4 Systematic Optimization of EVs applying Box-Behnken Design (BBD)

For the systematic optimization of BM seed oil-loaded EVs and to acquire precise mathematical data, a 3-factor, 3-level BBD was used. BBD recommended the preparation of 17 formulations for BM seed oil-loaded EVs. The input variables were the concentration of seed oil (X_1), concentration of phospholipid (X_2) and concentration of ethanol (X_3), while the response variables were particle size, %EE, and PDI. According to the BBD, all of the independent and response variables are listed as shown in Table 7 (BM seed oil-loaded EVs).

Table 7
Obtained values of BM seed oil-loaded EVs from 17 formulations run under BBD

Runs	BM Oil conc. (%)	PL90Gconc. (%)	Ethanol conc. (%)	Particle size (nm)	%EE	PDI
1	10	10	25	252	96.8	0.304
2	10	7.5	17.5	292.5	90.7	0.307
3	10	7.5	17.5	292.5	90.7	0.307
4	10	7.5	17.5	292.5	90.7	0.307
5	15	7.5	10	633.3	57	0.457
6	5	5	17.5	298.0	88.7	0.337
7	10	5	25	550.0	68.9	0.466
8	5	7.5	25	410.8	77.2	0.421
9	10	5	10	446.8	71.2	0.434
10	15	7.5	25	249.0	98.9	0.301
11	10	7.5	17.5	292.5	90.7	0.307
12	10	7.5	17.5	292.5	90.7	0.307
13	5	10	17.5	285.4	93.3	0.304
14	15	5	17.5	324.1	88.1	0.321
15	5	7.5	10	380	83.3	0.344
16	10	10	10	470	70.4	0.446
17	15	10	17.5	340	84.4	0.343

3.4.1 Model Generation of BM seed oil-loaded EVs

Polynomial expressions of the type as given in Eq. 1 were generated for the analysed response parameters, vesicle size, PDI, and %EE. Coefficients were also estimated for each response with β_0 as the intercept. The designs were also discovered to have insignificant values of "lack of fit," implying that the proposed design was adequate.

$$\beta_0 + X_1 + X_2 + X_3 + X_1X_2 + X_1X_3 + X_2X_3 + X_1^2 + X_2^2 + X_3^2 \quad (1)$$

Using ANOVA, the models for particle size, PDI, and %EE response variable were found to be extremely significant ($p < 0.05$). The r^2 value of the model was 0.98, indicating that the RSM polynomials satisfy the response variable statistics well.

The proximity of adjusted r^2 to actual model r^2 implied remarkable fit to the data. The design was found to have outstanding "lack of fit" values, confirming the validity of the hypothesised model.

3.4.2 Model Analysis of BM seed oil-loaded EVs

Model Diagnostics of BM seed oil-loaded EVs

Figures 3 (a-c) show normal plots of residuals versus normal percent probability and internally studentized residuals for vesicular size, PDI, and %EE. These plots demonstrate whether or not the residuals have a normal distribution. All of the investigated responses (vesicular size, PDI, and %EE) accompanied a linear trend, demonstrating that the model was capable of providing astonishingly adequate analysis and thus no transition was required.

Figure 4 (a-c) shows the residuals versus experimental run order plots for vesicle size, PDI, and %EE, respectively. This plot investigates the hidden variables that may have an effect on the experiment's response. In all of the studied response variables (vesicle size, PDI, and %EE), points were evenly split between the limit lines in a stable range, implying that the order of runs was capable of ensuring effective randomization and the model was able to identify the hidden variables.

The response value plots between predicted and actual response values for particle size, PDI and %EE respectively are shown in Fig. 5 (a-c). This type of plot is useful for determining values or groups of values that are not entirely predictable by the design being used. In the case of vesicle size, points near the diagonal line demonstrated that the design could interpret the results.

Box-Cox plots for vesicle size, PDI, and %EE are shown in Fig. 6 (a-c). This plot can assist you in determining the best power law transition. The lambda 'l' value, that is the least extremity of the curve created by the natural log of the overall squares of the residuals, is the recommended transition. There is no need for transition if the 95% significance level around the lambda includes 1. However, if it is -1, 0, or 0.5, an opposite, natural log, or square root design transition is essential. The design estimated the lambda value for vesicle size, so no transition was needed.

3.5 Response surface mapping of BM seed oil-loaded EVs

Figures 8 show the response surface representation that was created to plot the response across the entire experimental zone. Figure 7 (a-c) shows particle size 2-D contour and 3-D response surface diagrams. The figures clearly show the importance of PL and seed oil concentration on vesicle formation. The linear relationship between PL and seed oil concentration with vesicle size was clearly portrayed in Fig. 7 (a). Figure 7 (b) portrayed the curvilinear effect of ethanol and seed oil concentration on vesicle size. This could be because an increase in concentration of ethanol first resulted in decline in the size of vesicles, followed by a modest increase. Figure 7 (c) shows how PL and ethanol have an outstanding effect on the size of vesicles. In the intermediate levels of ethanol, there is a slight fall off followed by a slight elevation, whereas as previously demonstrated, PL conc. influences particle size in a linear fashion, there is a sharp increase in vesicle size as PL conc. increases.

Figure 7 (d-f) represents the %EE 2-D contour and 3-D response surface representation. However, while all of the input variables had a definite consequence on the %EE, PL concentration had a more pronounced effect. The %EE increased in proportion to the increase in PL and ethanol concentration. This could be due to increased entrapment of the lipophilic drug (i.e., BM seed oil) inside the PL membranes.

Figure 7 (g-i) represents the PDI 2-D contour and 3-D response surface representation. Almost all of the input variables had a definite consequence on PDI at all levels. Minimum PDI values were found at intermediate levels of all three factors.

3.6 Model optimization and validation of BM seed oil-loaded EVs

The search for ideal BM seed oil-loaded EVs was achieved using numerical optimization and the desirability feature to achieve the specified objectives for the response variables. The range of desired characteristics to achieve the most optimised EVs formation was fixed as constraints. The entire experimental domain was examined for ideal constituents with the maximum responses that met the predefined constraints (Singh et al. 2005). The desirability function, 'r' similar or equivalent to unity, was designated as a predictor of the right fit constituents with desirable characteristics. Tables 8 and 9 enlist various constraints and predicted solutions of numeric optimization for BM seed-oil loaded EVs, as well as their numerical range of desirability.

The prepared formulations of BM seed oil-loaded EVs was chosen according to the standard, i.e., minimal value for particle size and PDI, maximal for %EE by applying constraints on Y_1 ($218.1 \leq Y \leq 633.3$); Y_2 ($0.287\ Y \leq 0.367$) and Y_3 ($18.2 \leq Y \leq 56$) respectively, to achieve a desirability function value near to 1. The RSM yielded a total of ten solutions of formulations of BM seed oil-loaded EVs. Seven formulations having highest desirability value (greater than 0.9) were subjected to check point analysis and the observed data compared to the predicted responses (Table 10). Linear correlation representation of the actual and predicted response variables [Figure 8 (a-c)] showed high values of r^2 (Particle size = 0.954; PDI = 0.955; and %EE = 0.937), designating outstanding goodness of fit. The cumulative bias for response variables was found to be -0.044 ± 0.096%, implying that the QbD experiments had a very high degree of prediction accuracy. It was discovered that the residual plots were highly constrained, with uniform, restrictive, and irregular disperse around the zero-axis.

The Solution selected as optimum formulation had low %error for all the three response variables and had a combination of appropriate response values, namely minimum particle size (249 nm), PDI (0.301) and %EE (53.84%).

Table 8
Constraints for numeric optimization for BM seed oil-loaded EVs

Variable	Goal	Lower limit	Upper limit	Importance
BM Seed oil concentration	In range	5	15	3
PL concentration	In range	5	10	3
Ethanol	In range	10	25	3
Particle Size	Minimize	218.1	633.3	3
EE%	Maximize	18.2	56	3
PDI	In range	0.287	0.367	1

Table 9
Predicted solutions of numeric optimization for BM seed-oil loaded EVs

BM Seed oil conc.	Lipid conc.	Ethanol	Particle size	PDI	%EE	
11.36	5.00	25.00	240.99	0.328	53.83	
11.32	5.00	25.00	249.15	0.302	53.94	**Selected**
11.40	5.00	25.00	238.60	0.329	53.80	
11.47	5.00	25.00	239.43	0.324	53.78	
11.07	5.11	24.99	237.41	0.324	52.99	
11.97	5.00	24.92	239.32	0.325	52.33	
11.72	5.00	25.00	238.15	0.323	53.66	

Table 10
Comparison of experimental and predicted responses

Response variables	Predicted	Observed	Residuals	%error
Particle size	240.99	239.69	1.3	0.542
	249.15	249.00	0.15	0.060
	238.6	239.03	-0.43	-0.179
	239.43	239.24	0.19	0.079
	237.41	238.42	-1.01	-0.432
	239.32	239.34	-0.02	-0.008
	238.15	238.64	-0.49	-0.205
PDI	0.328	0.327	0.001	0.305
	0.302	0.301	0.001	0.331
	0.329	0.33	-0.001	-0.303
	0.324	0.323	0.001	0.324
	0.325	0.323	0.002	0.619
	0.323	0.32	0.003	0.937
%EE	53.83	53.68	0.15	0.279
	53.94	53.84	0.10	0.188
	53.8	53.79	0.01	0.018
	53.78	53.77	0.01	0.018
	52.99	52.97	0.02	0.037
	52.33	52.49	-0.16	-0.304
	53.66	53.6	0.06	0.111

3.7 Preparation of BM seed oil-loaded ethanolic vesicular hydrogel

The optimized BM seed oil-loaded EVs were refrigerated till further use as shown in Fig. 9 (Ma et al., 2018).

The optimised BM seed oil-loaded EVs was incorporated into the carbopol. At low concentrations, carbopol 934 forms a very fine consistency transparent gel. The prepared BM seed oil-loaded EVs were

gradually added to the carbopol 934 gel base with gentle stirring to form the gel as shown in Fig. 10 (Patel et al., 2012).

3.7.1 Characterization of the BM seed oil-loaded EVs

Particle size of BM seed oil-loaded EVs

The average particle size of BM oil-loaded EVs was determined based on the measurements of different batches of EVs. The particle size of optimised formulation was 249.0 nm and PDI was 0.301.The PDI of all the EVs was found to be below 0.4 which proved narrow size distribution of vesicles as portrayed in Fig. 11.

Percent entrapment efficiency (%EE)

It has been demonstrated that the drug may alter lipid vesicle production. According to this research, the impact of concentration of ethanol on phospholipidic vesicles is dependent on a variety of parameters, including manufacturing process, drug loading type, and phospholipid concentration. The % EE of the EVs was shown to rise with increasing content of ethanol. As ethanol was disseminated throughout the vesicles, the higher %EE might be explained by improved drug solubility in the centre together with lamellar of the EVs (Sakdiset et al., 2019).

%EE of EVs was measured to check the ability of the EVs to encapsulate the drug. %EE of BM seed oil-loaded EVs was in the range of 50–99%. The formulations containing higher amount of ethanol revealed higher %EE.

HR-TEM of BM seed oil-loaded EVs

The BM seed oil-loaded EVs prepared were uniform rhombic dodecahedral shaped vesicles and were found to be smooth and regular with the magnification of 10000X as portrayed in Fig. 12 displaying the sealed vesicular composition. Some particle shapes that deviate from sphericity may be due to lipid alteration during the sample treatment process. Furthermore, the particle shape is determined by the purity of the lipid.

FESEM of BM seed oil-loaded EVs

The images of the optimized BM seed oil-loaded EVs displayed spherical shaped isolated vesicles. The surface of the vesicles was smooth, which was confirmed by FESEM with the magnification of 1000X as portrayed in Fig. 13.

3.8 Characterisation of BM seed oil-loaded ethanolic vesicular hydrogel

3.8.1 Rheology

Rheological analysis can be used to help determine the potential of novel pharmaceutical formulations. The rheograms for all ethanolic vesicular hydrogels showed non-Newtonian pseudoplastic flows. The shear rate influences viscosity. In other words, typical properties of ethanolic vesicular hydrogels are observed as shear rate increases with increasing shear stress.

The rheogram of BM seed oil-loaded ethanolic vesicular hydrogel is depicted in Fig. 14. Value of “n” was found to be 0.278 which is less than 1, designating the ethanolic vesicular hydrogel to be of shear-thinning nature as shown in Fig. 14. Apparent viscosity of BM seed oil-loaded ethanolic vesicular hydrogel was 5970 Pa.s and yield value obtained was i.e. 298, which may be attributed to the sternness of the structure of hydrogel of the ethanolic vesicular hydrogel, thus necessitating elevated shear to start off its stream as represented in Fig. 15.

3.9 Minimum Inhibitory Concentration (MIC)

The broth microdilution assay for determining the MIC of antifungal agents for yeasts, was used to assess, the antifungal activity of BM seed oil, BM seed oil-loaded EVs and ethanolic vesicular hydrogel against *C. albicans* as shown in Table 11 and Fig. 16. This method allows for determination of the MIC for *C. albicans* strain in µg/mL (Nenoff et al., 2016).
In the case of BM seed oil-loaded EVs and ethanolic vesicular hydrogel there was 2.5 times each reduction in MIC values vis-à-vis against *C. albicans.*

This could be due to improved interactions between the EVs and fungal cells, wherein due to the enhanced permeation of seed oils through EVs, across the fungal cell walls, might have restricted the ergosterol synthesis (Raza et al., 2013).

Table 11
MIC of BM seed oil, BM seed oil-loaded EVs, ethanolic vesicular hydrogel

Formulations (BM)	MIC (mg/mL)
BM seed oil	0.0125
BM seed oil loaded EVs	0.00078125
Ethanolic vesicular hydrogel	0.00078125
Fluconazole (+ ve)	0.003125

3.10 Anti candida activity by agar well diffusion method: Antic*andida* activities of BM seed oil, BM seed oil-loaded EVs and ethanolic vesicular hydrogel were assayed against *C. albicans* isolates by agar well diffusion (Nejad et al., 2013). Clear zone of inhibition was observed showing antifungal activity against *Candida* strain of (ATCC 90028) as shown in Table 12 and in Fig. 17.

Table 12
Zone of inhibition of BM seed oil, BM seed oil-loaded EVs and ethanolic vesicular hydrogels

Formulations	Diameter of Clear zone of inhibition (in mm)
	BM
Seed oil- loaded EVs	19
Ethanolic vesicular hydrogel	20
Seed oil	19
Positive control (Fluconazole)	21

3.11 Vaginal candidiasis mice model for *in vivo* studies

The skin photographs of mouse vaginal skin surface treated with BM seed oil-loaded formulations on different days are depicted in the Fig. 19.

Different scores ranging between 0 and 5, were assigned to these formulation-treated vaginal skin photographs, according to the inflammation extent as shown in Table 13 and the Figs. 18. Inflammation extent as was scored as: a) absent (score of 0), meaning no swelling, vaginal discharge, and redness, b) mild (score of 1–3) meaning mild redness and swelling with no vaginal discharge, c) moderate (score of 3–4), meaning moderate swelling, redness, and vaginal discharge, d) severe (score of 5), meaning sufficient swelling, redness and vaginal discharge.

Table 13
Inflammation extent on a score of 0–5

Treatment groups	Inflammation extent (scores of 0–5)		
	Day 1	Day 2	Day 3
BM seed oil	4	3	2.5
BM seed oil-loaded EVs	4	2.5	0
BM seed oil-loaded ethanolic vesicular hydrogel	3	1.5	0.5
Marketed cream (clotrimazole)	3	2	0
Negative control	0	0	0
Positive control	5	5	5

Inflammation scores for vaginal candidiasis mice model treated with various BM oil-loaded formulations. Negative controls is mice without vaginal candidiasis infection, positive control is mice with vaginal candidiasis infection but no treatment. The treatment groups were BM seed oil, BM seed oil-loaded EVs, BM seed oil-loaded ethanolic vesicular hydrogel formulation, and marketed formulation. The statistical

analyses, was performed by using one-way ANOVAs with Tukey- Multiple Comparisons tests having p value < 0.05. Standard deviations are represented by the error bars.

BM seed oil-loaded EVs and ethanolic vesicular hydrogel decreased the vaginal fungal burden to a similar extent as topical marketed drug (clotrimazole) as shown in Fig. 19. This could be interpreted by analysing the decrease in severity of symptoms like: vaginal discharge, swelling and inflammation.

3.12 Histopathology analysis of vaginal tissues

Anti*candida* potency of BM seed oil, BM seed oil-loaded EVs and ethanolic vesicular hydrogel were compared with BM seed oil, marketed cream (clotrimazole), negative and positive control. Skin histology revealed dynamic alterations during the planned treatment protocol as shown in Fig. 20 (a-f).

Histopathological analysis of vaginal tissue of the group treated as positive control showed very heavy inflammation in epithelium as shown in Fig. 20 (a), BM seed oil showed moderate to mild neutrophils in epithelium and sub-epithelium as shown in Fig. 20 (b), BM seed oil-loaded EVs showed reduced inflammation in epithelium as shown in Fig. 22 (c). The ethanolic vesicular system distorts and fluidizes the vaginal layer, allowing the soft vesicle to fuse and leak its drug content inside the contaminated fungal cells (Touitou and Natsheh, 2021). The expanding accumulation of BM seed oil within the skin via ethanolic vesicular carrier may aid in optimising drug targeting to the vaginal layer, opening up new avenues for well-controlled and modern application to the skin of BM seed oil for treating various fungal infections (Verma and Pathak, 2012). Ethanolic vesicular hydrogel showed no or very mild inflammation as shown in Fig. 20 (d). The histological samples of the optimised ethanolic vesicular hydrogel and the marketed cream were nearly identical. They demonstrated skin structure same as the skin treated with the negative control (Elnaggar et al., 2016). Marketed formulation (clotrimazole) showed mild inflammation with presence of very few neutrophils as shown in Fig. 22 (e). Negative control showed no inflammation as portrayed in Fig. 20 (f).

The results of the *in vivo* analyses indicated that the sustained and increased antifungal potential could be attributed to the accumulation of components of the ethanolic vesicular hydrogel into the vaginal layer, thereby improving the capacity of drug retention in the vaginal layers (Kenechukwu et al., 2017).

4. Conclusion

In the present work, EVs were chosen as carrier systems for the topical delivery of BM seed oil. BM seed oil-loaded EVs were developed by employing Box-Behnken design (BBD) which proved to a very effective tool in optimization of formulation. FESEM images of BM seed oil-loaded EVs showed the vesicles to be of uniform rhombic dodecahedral shape possessing smooth surface and sealed vesicular structure. The antifungal activity of BM seed oil-loaded EVs and ethanolic vesicular hydrogel showed marked improvement in comparison to that of plain BM seed oil. This could be due to improved interactions between the EVs and fungal cells.

In vivo studies reflected the ability of ethanolic vesicular hydrogel to reduce inflammation to a greater extent in comparison to other treatment groups. Better antifungal activity of the EVs may be attributed to enhanced penetration of the lipid particles containing BM oil through fungal cell walls to inhibit ergosterol synthesis.

The work overall reveals the importance of ethanolic vesicular nano-range carrier systems in improving the antifungal activity against *C. albicans*. It may be inferred that the developed BM seed oil-loaded EVs and ethanolic vesicular hydrogel can effectively improve the management of vaginal candidiasis in animal model by providing good vehicular support to the seed oil for better permeation, retention and contact time with the vaginal skin. Further this formulation maybe evaluated preclinically in more advanced animal models and at clinical levels for overall benefit of the society. From these performed studies, it can be concluded that the BM seed oil-loaded EVs and ethanolic vesicular hydrogel can be explored as a potential alternative herbal product for vaginal candidiasis.

Declarations

Authors' Contributions Conceptualisation, PN, AS, and AP; Methodology, PN, AS; Validation, AnS, SA, KD, DKC; Formal analysis, PN, SA, SKS, GG; Investigation, PN, AS, AnS, AP; Data curation, PN, GG, SKS ; writing, original draft preparation, AS, PN, SA; writing,review and editing, PN, SA, KD, DKC; Visualisation, PN, AS, AP; Supervision, PN, SA; Project administration, PN, AnS, KD; and Funding acquisition, NONE.

Data Availability All data would be available on request.

Ethical approval Approval for use of animals was granted by IAEC of Shoolini University, Solan.

Competing interests The authors declare no competing interests.

Funding No funds, grants or other support was received.

Acknowledgement The authors would like to thank School of Pharmaceutical Sciences, Shoolini University, Solan for providing the necessary facilities and support for carrying out the work.

References

1. Ascenso A, Raposo S, Batista C, Cardoso P, Mendes T, Praça FG, et al. (2015) Development, characterization, and skin delivery studies of related ultradeformable vesicles: transfersomes, ethosomes, and transethosomes. Int J Nanomed 10:5837.
2. Chauhan SS, Mahish PK. (2020) Flavonoids of the flame of forest-Butea monosperma. Res J Pharm Tech 13(11):5647-53.
3. Cupara S, Jankovic S, Arsic I, Tadic V, Jarcevic V(2012) Characterization of seabuckthorn oil emulsion. Mil Med Sci Lett (VojZdravListy) 81:56-60.

4. Elnaggar YS, Talaat SM, Bahey-El-Din M, Abdallah OY (2016) Novel lecithin- integrated liquid crystalline nanogels for enhanced cutaneous targeting of terconazole: development, in vitro and in vivo studies. Intl J Nanomed 11:5531.
5. Garg NK, Sharma G, Singh B, Nirbhavane P, Tyagi RK, Shukla R, et al. (2017) Quality by Design (QbD)-enabled development of aceclofenac loaded-nano structured lipid carriers (NLCs): An improved dermatokineticprofile for inflammatory disorder (s). Int J Pharmaceutics 517(1- 2):413-31.
6. Gonçalves B, Ferreira C, Alves CT, Henriques M, Azeredo J, Silva S (2016) Vulvovaginal candidiasis: Epidemiology, microbiology and risk factors. Critical Rev Microbiol 42(6):905-27.
7. Indora N, Kaushik D. Design, development and evaluation of ethosomal gel of fluconazole for topical fungal infection. Int J Engg Sci Invention Res Develop 1(8):280-306.
8. Ismail TA, Shehata TM, Mohamed DI, Elsewedy HS, Soliman WE (2021) Quality by design for development, optimization and characterization of brucine ethosomal gel for skin cancer delivery. Molecules 26(11):3454.
9. Ito H, Asmussen S, Traber DL, Cox RA, Hawkins HK, Connelly R, et al. (2014) Healing efficacy of sea buckthorn (Hippophaerhamnoides L.) seed oil in an ovine burn wound model. Burns 40(3):511-9.
10. Kenechukwu FC, Attama AA, Ibezim EC, Nnamani PO, Umeyor CE, Uronnachi EM, et al. (2017) Tailor-made mucoadhesive lipid nanogel improves oromucosal antimycotic activity of encapsulated miconazole nitrate. Eur J Nanomed 9(3-4):115-26.
11. Kırıcı P, Kaplan S, Turk BA, Annac E (2021) Histopathological Examination of the Mucosal Effects of Obstetric Gel on Vaginal Wound Healing in an Incision- Inflicted Rat Model. Cureus13(9).
12. Limsuwan T, Amnuaikit T (2012) Development of ethosomes containing mycophenolic acid. Procedia Chemistry 4:328-35.
13. Ma H, Guo D, Fan Y, Wang J, Cheng J, Zhang X (2018) Paeonol-loaded ethosomes as transdermal delivery carriers: design, preparation and evaluation. Molecules 23(7):1756.
14. Mahmood S, Mandal UK, Chatterjee B, Taher M (2017) Advanced characterizations of nanoparticles for drug delivery: investigating their properties through the techniques used in their evaluations. Nanotech Rev 6(4):355- 72.
15. Negi P, Aggarwal M, Sharma G, Rathore C, Sharma G, Singh B, et al. (2017) Niosome-based hydrogel of resveratrol for topical applications: An effective therapy for pain related disorder (s). Biomed Pharmacotherp 88:480-7.
16. Negi P, Singh B, Sharma G, Beg S, Katare OP(2015) Biocompatible lidocaine and prilocaine loaded-nanoemulsion system for enhanced percutaneous absorption: QbD-based optimisation, dermatokinetics and in vivo evaluation. J Microencap 32(5):419-31.
17. Nenoff P, Krüger C, Neumeister C, Schwantes U, Koch D (2016) In vitro susceptibility testing of yeasts to nystatin–low minimum inhibitory concentrations suggest no indication of in vitro resistance of Candida albicans, Candida species or non-Candida yeast species to nystatin. Clin Med Investig 1:71-6.

18. Patel KK, Kumar P, Thakkar HP (2012) Formulation of niosomal gel for enhanced transdermal lopinavir delivery and its comparative evaluation with ethosomal gel. The American Association of Pharmaceutical Scientists Pharmscitech 13:1502-10.
19. Pathan İ (2016) Transdermal delivery of ethosomes as a novel vesicular carrier for paroxetine hydrochloride: in vitro evaluation and in vivo study. Marmara Pharmaceutical J 20(1):1-6.
20. Raza K, Singh B, Singla S, Wadhwa S, Garg B, Chhibber S, et al. (2013) Nanocolloidal carriers of isotretinoin: antimicrobial activity against Propionibacterium acnes and dermatokinetic modeling. Molecular Pharmaceutics 10(5):1958-63.
21. Safwat S, Ishak RA, Hathout RM, Mortada ND (2017) Nanostructured lipid carriers loaded with simvastatin: effect of PEG/glycerides on characterization, stability, cellular uptake efficiency and in vitro cytotoxicity. Drug Develop Industrial Pharm 43(7):1112-25.
22. Sakdiset P, Amnuaikit T, Pichayakorn W, Pinsuwan S (2019) Formulation development of ethosomes containing indomethacin for transdermal delivery. J Drug Deliv Sci Tech 52:760-8.
23. Shukla R, Tiwari G, Tiwari R, Rai AK (2020) Formulation and evaluation of the topical ethosomal gel of melatonin to prevent UV radiation. J Cosmetic Dermatol 19(8):2093-104.
24. Singh B, Mehta G, Kumar R, Bhatia A, Ahuja N, Katare OP (2005) Design, development and optimization of nimesulide-loaded liposomal systems for topical application. Curr Drug Deliv 2(2):143-53.
25. Soumya SL, Nair BR (2012) Antifungal efficacy of Capsicum frutescens L. extracts against some prevalent fungal strains associated with groundnut storage. Int J Agricul Techn 8(2):739-50.
26. Srivastava N, Patel DK, Rai VK, Pal A, Yadav NP (2018) Development of emulgel formulation for vaginal candidiasis: Pharmaceutical characterization, in vitro and in vivo evaluation. J Drug Deliv Sci Tech 48:490-8
27. Sutariya BK, Saraf MN (2015) A Comprehensive review on pharmacological profile of Butea monosperma (Lam.) Taub. J Appl Pharmaceutical Sci 5(9):159-66.
28. Tiwari P, Jena S, Sahu PK (2019) Butea monosperma: phytochemistry and pharmacology. Acta Scietific Pharmaceutical Sci 3(4):19-26.
29. Touitou E, Dayan N, Bergelson L, Godin B, Eliaz M (2000) Ethosomes—novel vesicular carriers for enhanced delivery: characterization and skin penetration properties. J Controlled Rel 65(3):403-18.
30. Verma P, Pathak K (2012) Nanosized ethanolic vesicles loaded with econazole nitrate for the treatment of deep fungal infections through topical gel formulation. Nanomed: Nanotech, Biol Med 8(4):489-96.
31. Walters D, Raynor L, Mitchell A, Walker R, Walker K. (2004) Antifungal activities of four fatty acids against plant pathogenic fungi. Mycopathologia 157:87- 90.
32. Wojciechowska K, Walczak A, Rostowska E, Poleszak E (2021) Comparison of sensory and rheological properties of green cosmetic creams prepared on different natural, ECOCERT and BDIH certificated self-emulsifying bases. Curr Issues Pharm Med Sci 34(4):218-23.

Figures

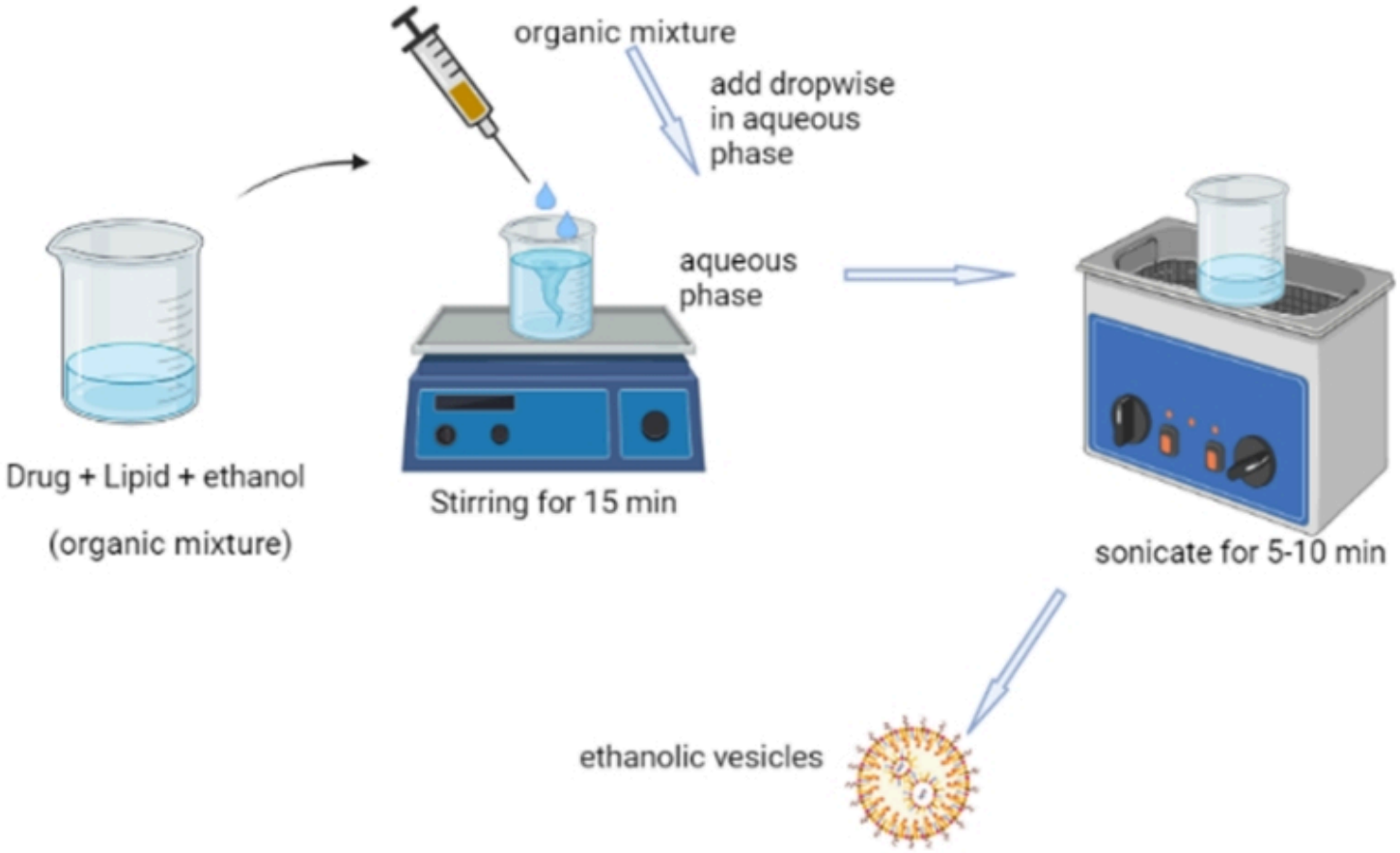

Figure 1

Schematic representation of preparation of BM seed oil-loaded EVs

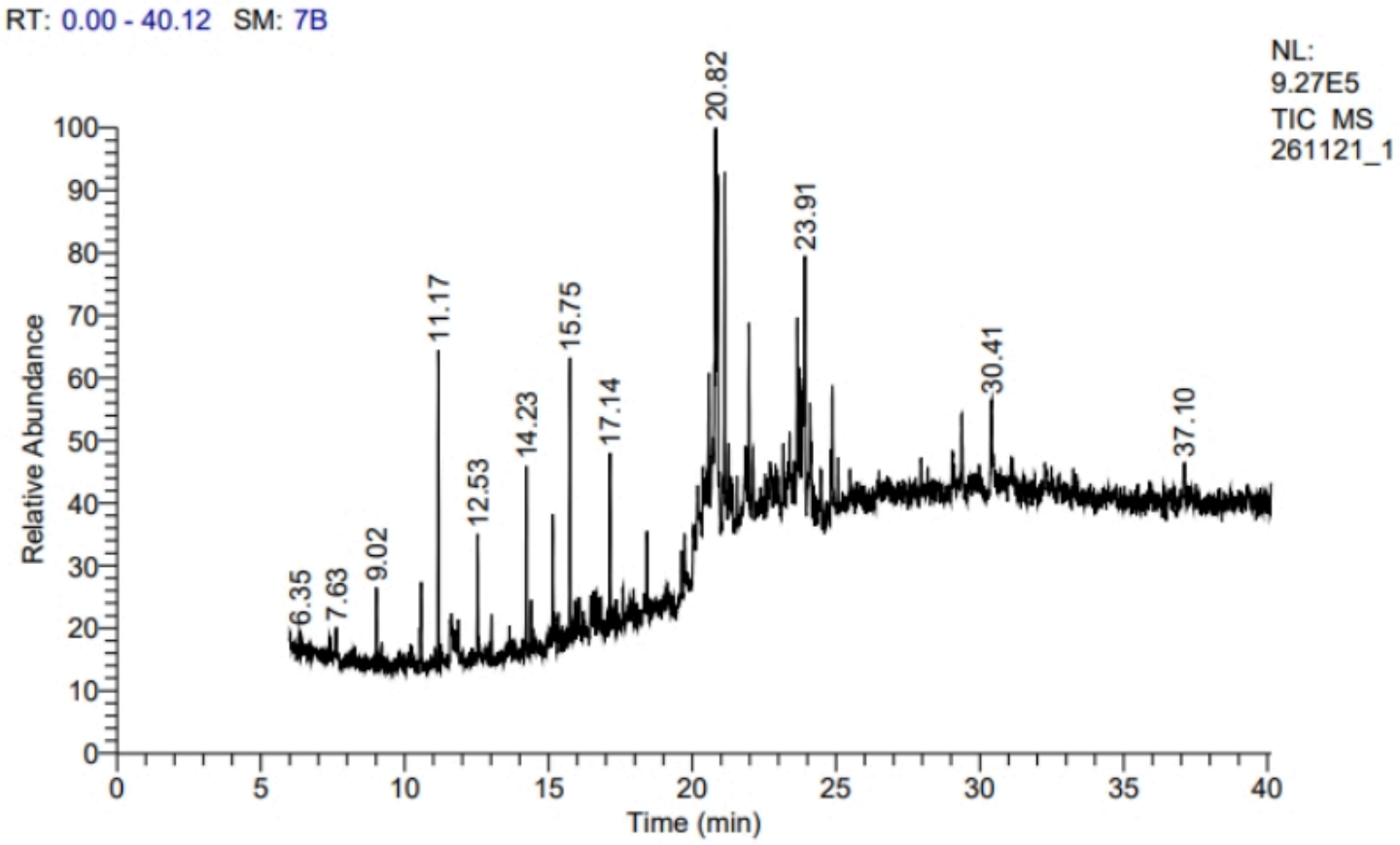

Figure 2

Chromatogram of BM seed oil

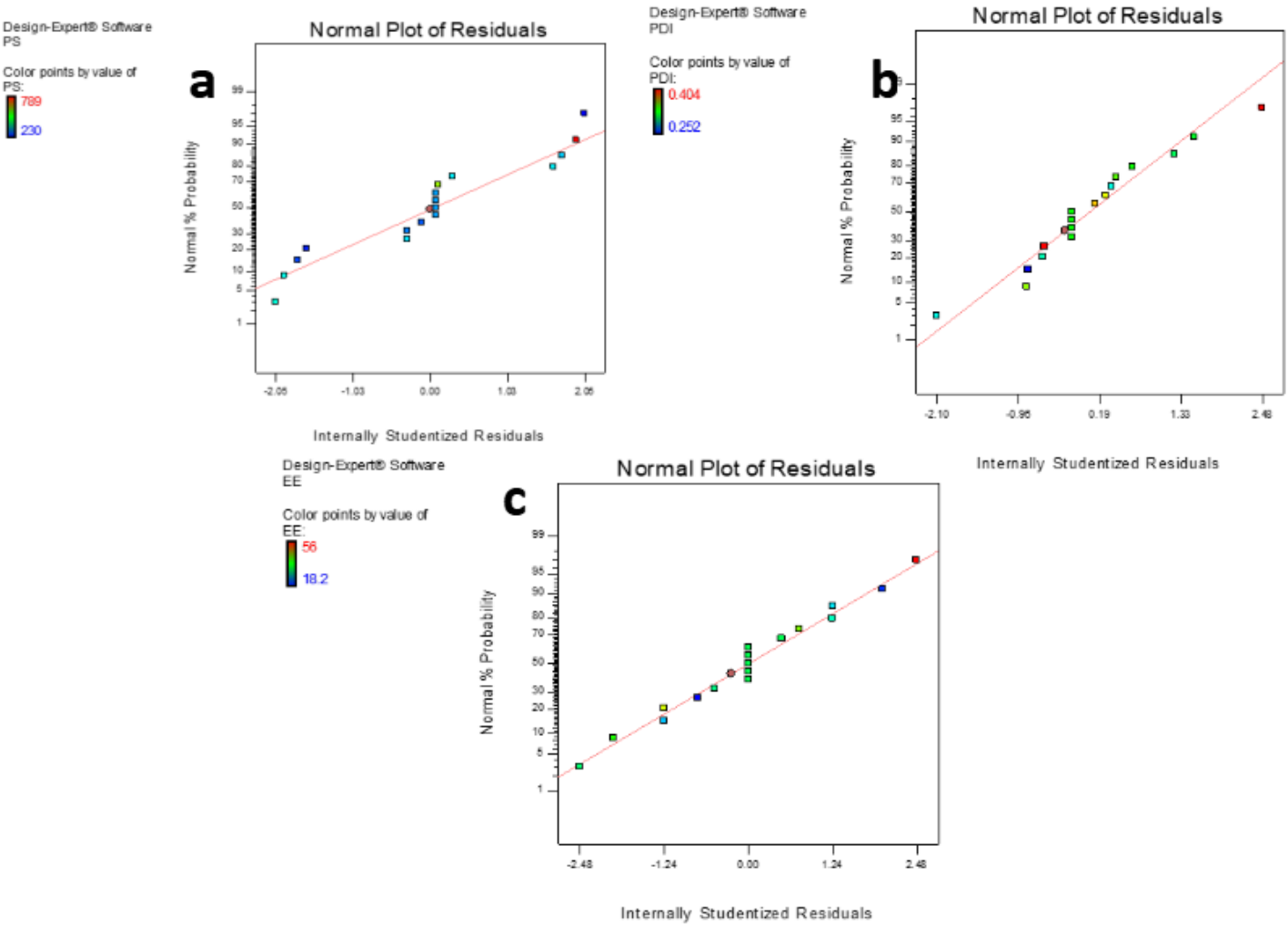

Figure 3

Normal plots of residuals; **(a)** Particle size; **(b)** PDI; **(c)** %EE

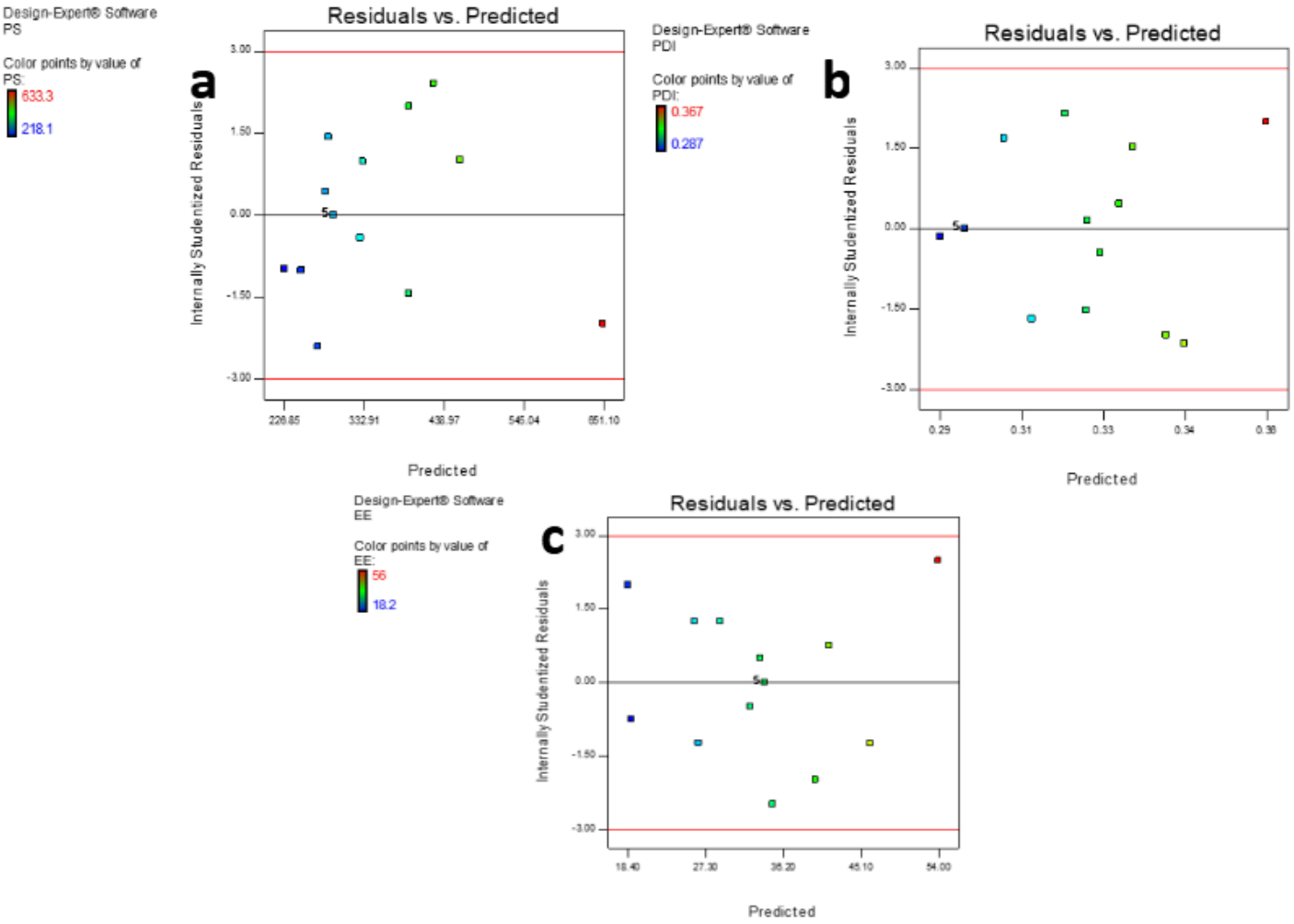

Figure 4

Residuals and predicted responses **(a)** particle size; **(b)** PDI; **(c)** %EE

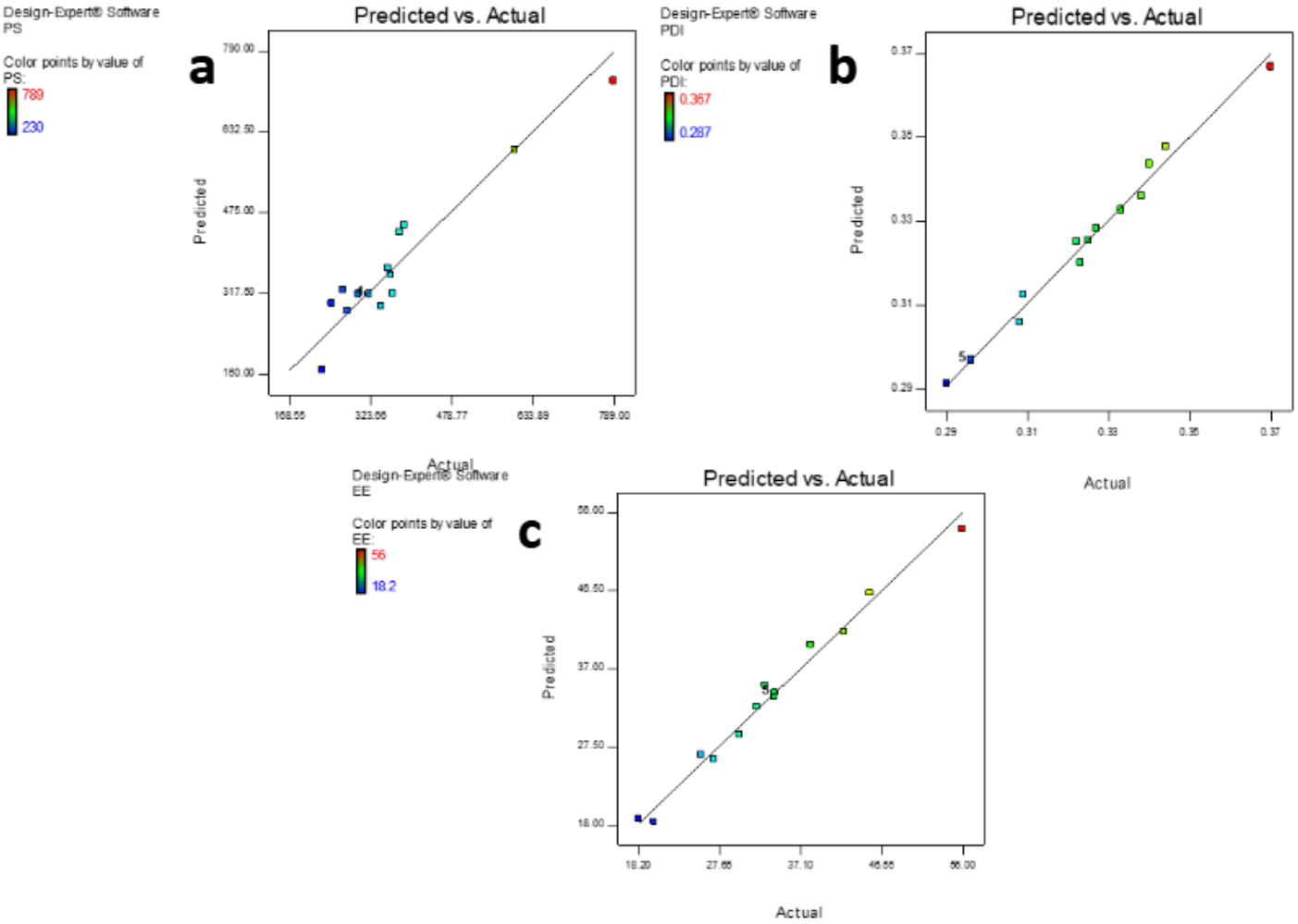

Figure 5

Predicted versus Actual Plots; **(a)** Particle Size; **(b)** PDI; **(c)** %EE

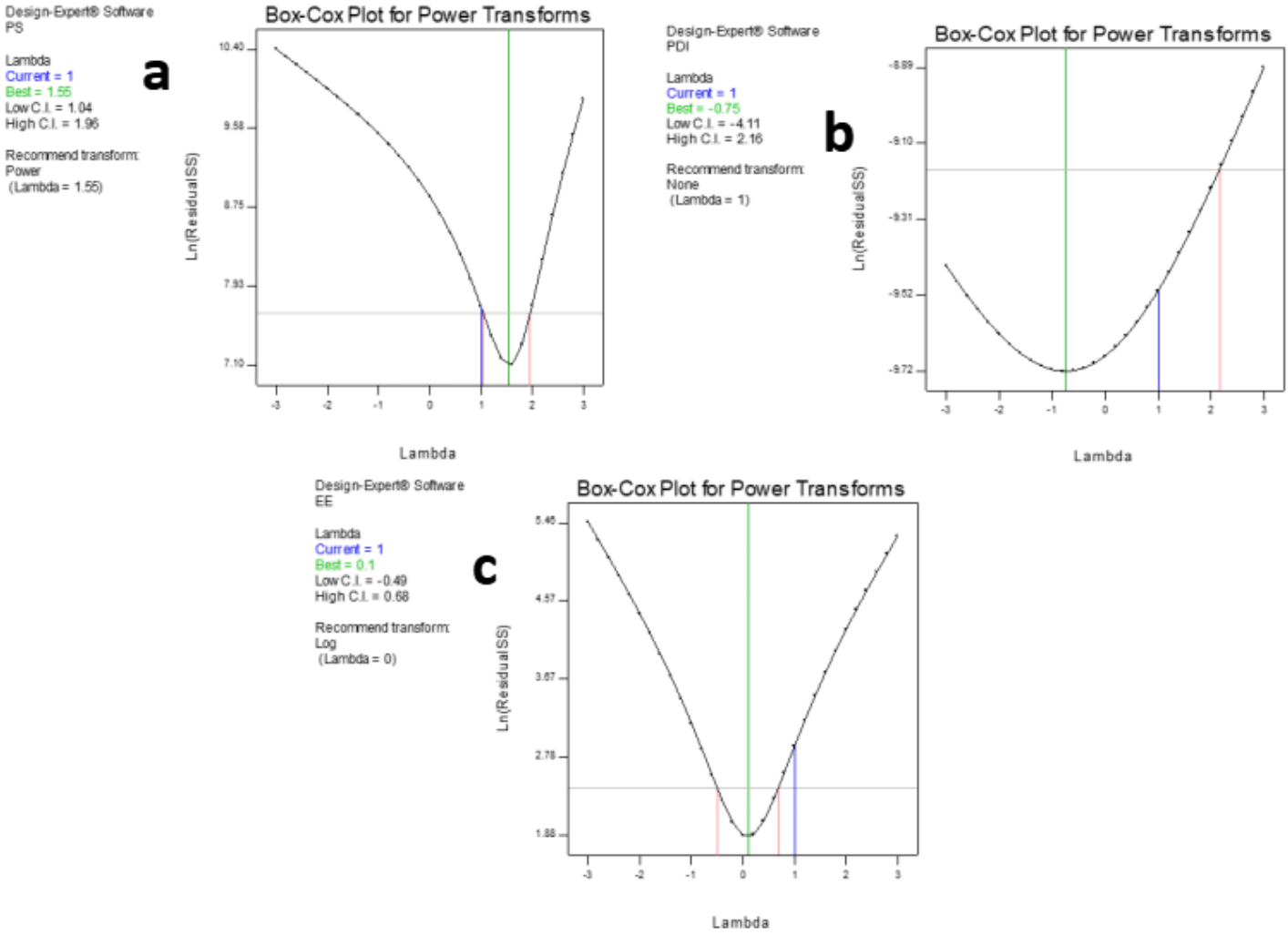

Figure 6

Power transformation Box-Cox plots **(a)** Particle size; **(b)** PDI; **(c)** %EE

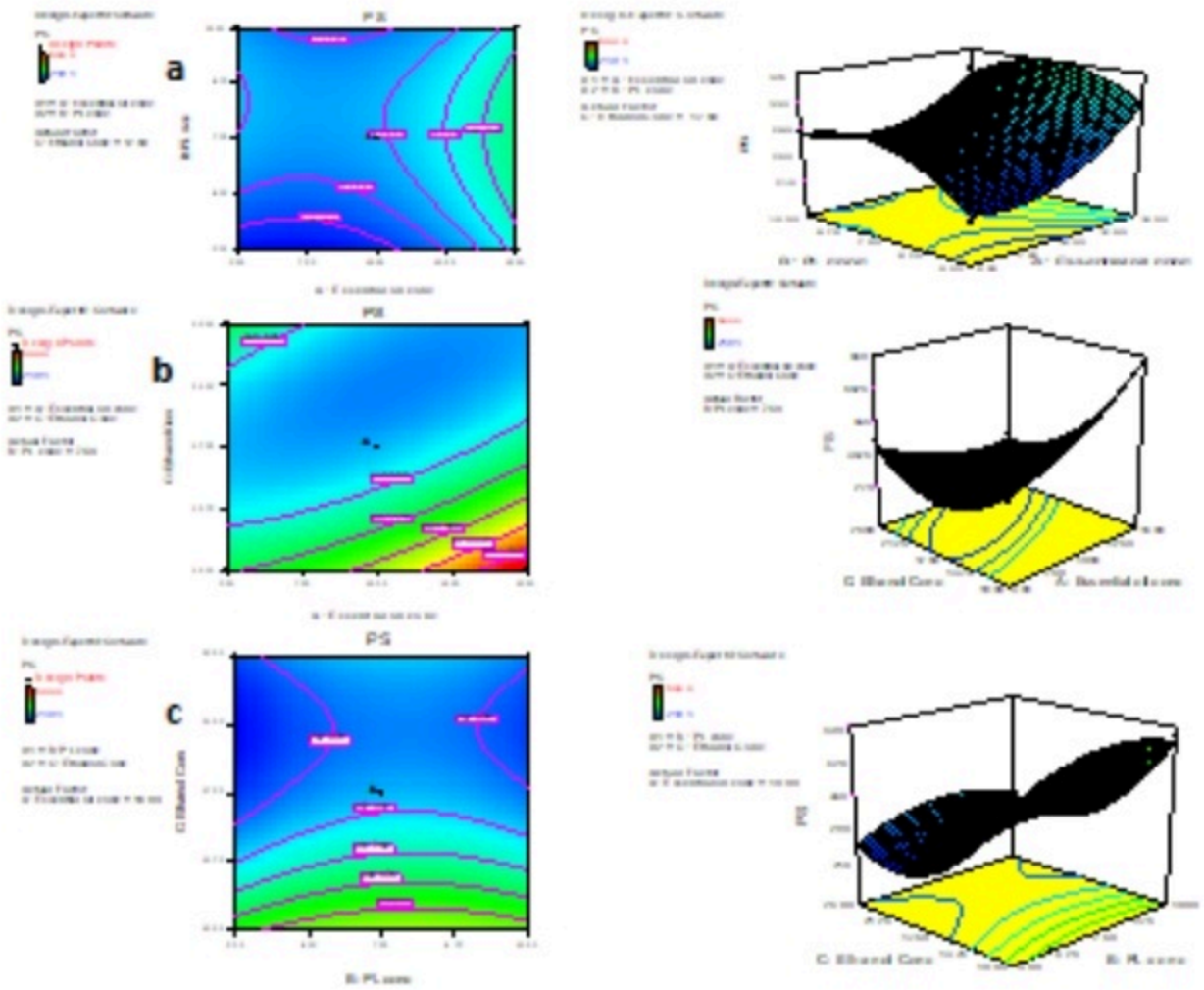

Figure 7

Figure 7 1. 2-D contour and three-dimensional response surface representation of BM seed oil-loaded EVs portraying the impact of various input variables on; Particle size; (a) Seed oil conc.(X_1), PL conc. (X2); **(b)** Seed oil conc. (X_1),Ethanol conc. (X_3); **(c)** PL conc (X_1), Ethanol conc. (X_3);

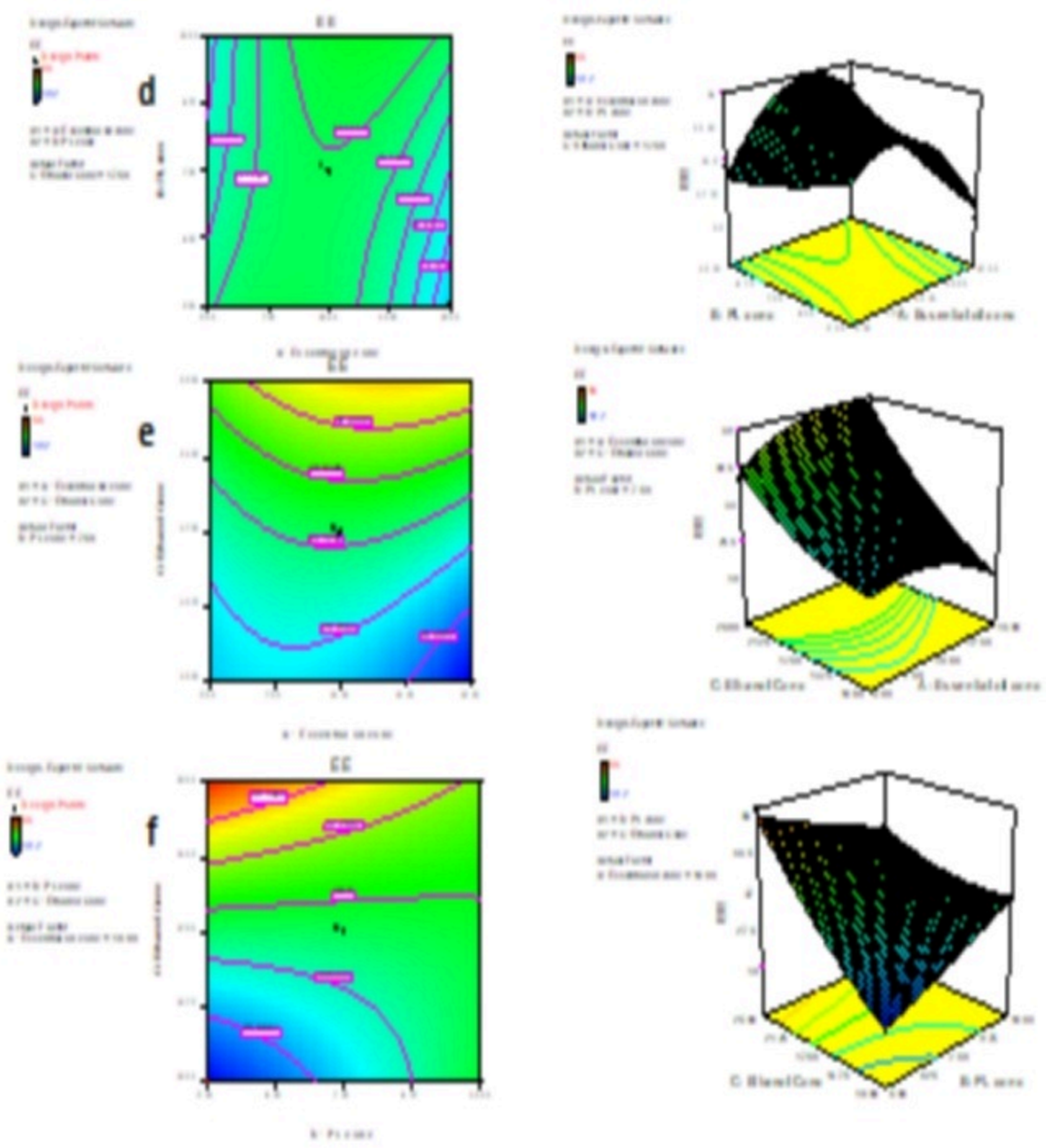

Figure 8

Figure 7 2. 2-D contour plots and 3-D response surface representation of BM seed oil-loaded EVs depicting the impact of various input variables on; %EE; **(d)** Seed oil conc.(X_1), PL conc. (X2); **(e)** Seed oil conc. (X_1),Ethanol conc. (X_3); **(f)** PL conc. (X_1), Ethanol conc. (X_3)

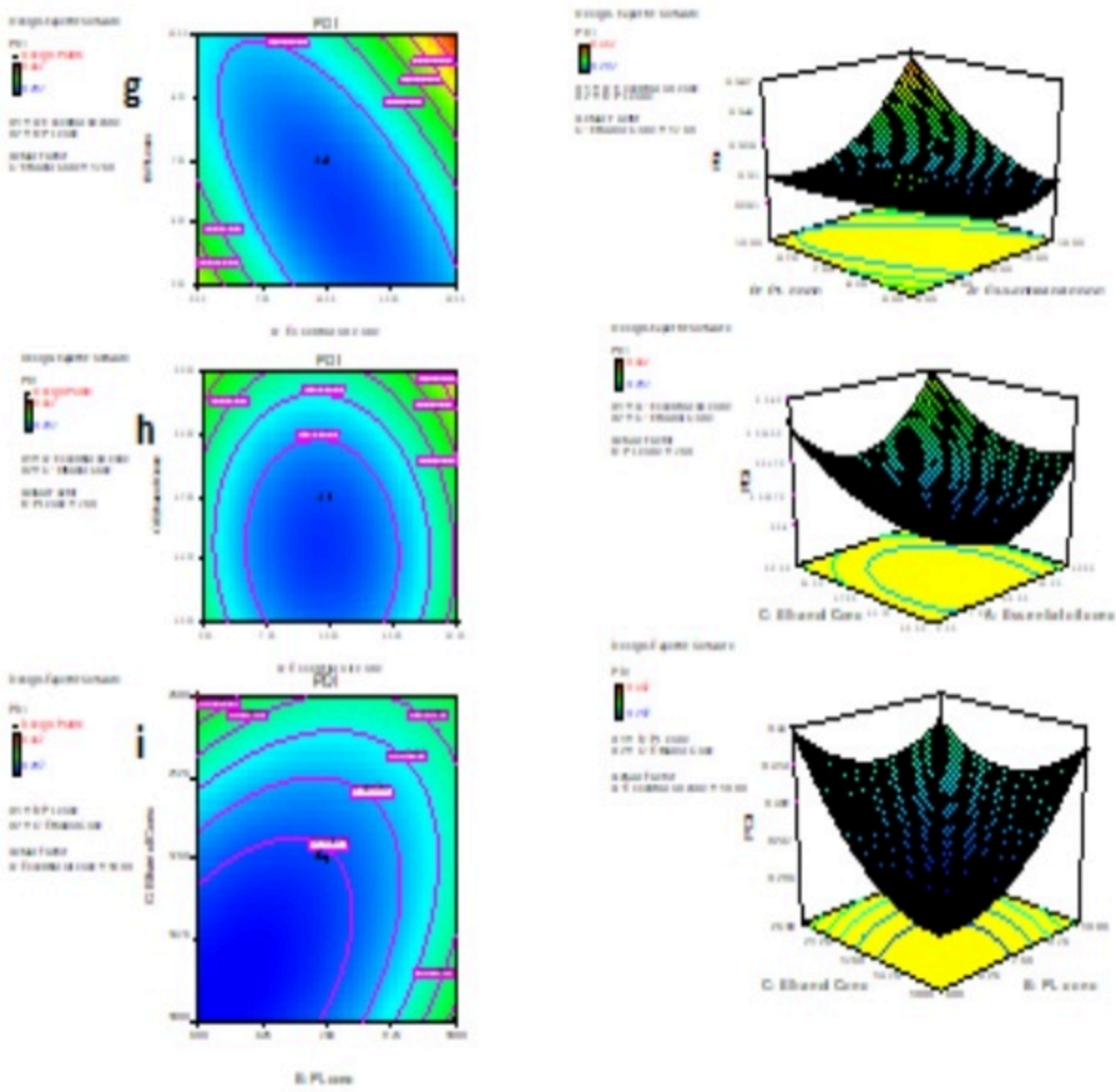

Figure 9

Figure 7 3. 2-D contour and 3-D response surface representation of BM seed oil-loaded EVs depicting the impact of various input variables on; PDI: (g) Seed oil conc.(X_1), PL conc. (X2); **(h)** Seed oil conc. (X_1), Ethanol conc. (X_3); **(i)** PL conc. (X_1), Ethanol conc. (X_3)

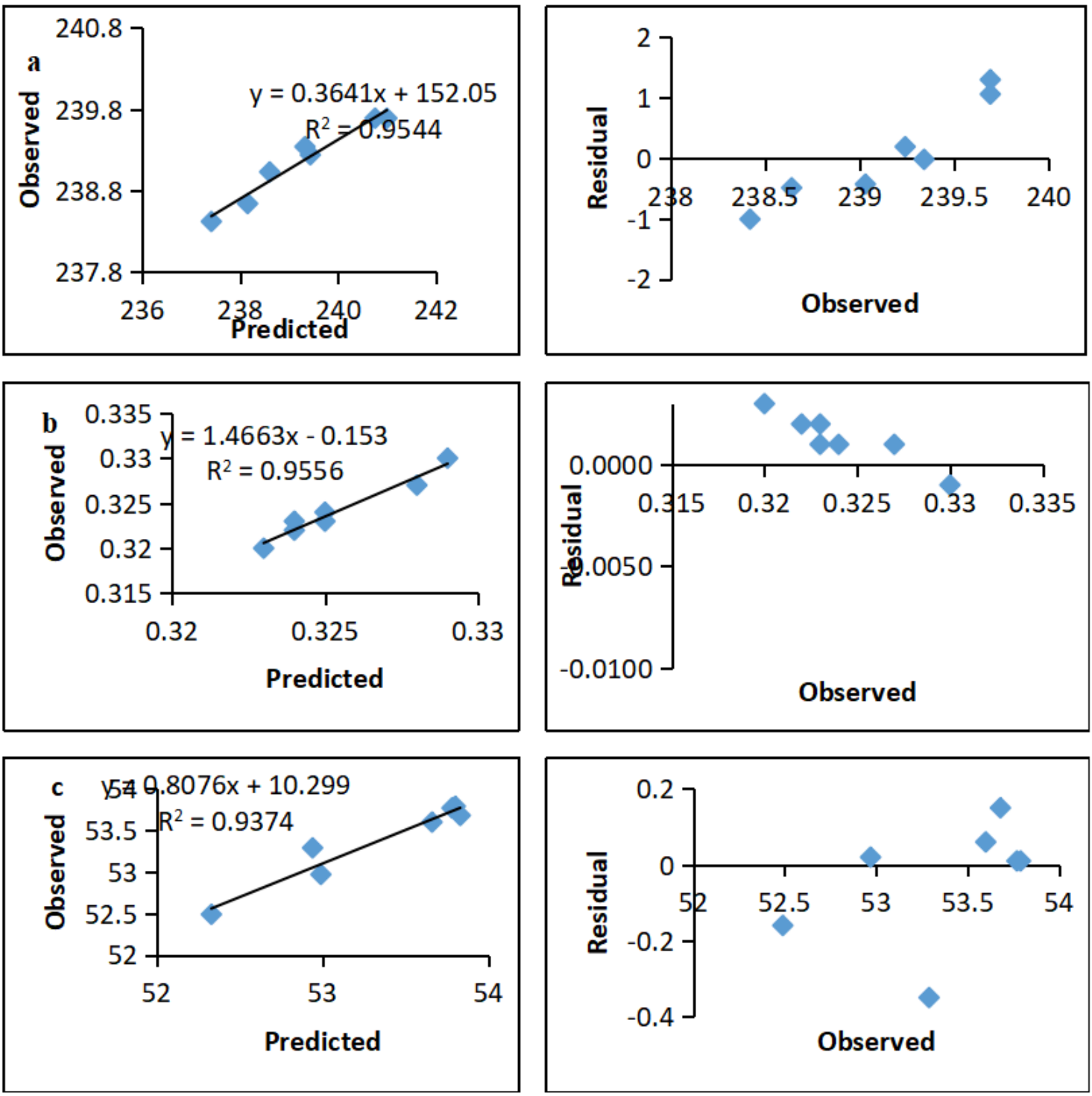

Figure 10

Figure 8 Representation between residuals and predicted values for BM seed oil-loaded loaded EVs, **a)** Particle size; **b)** %EE and **c)** PDI respectively

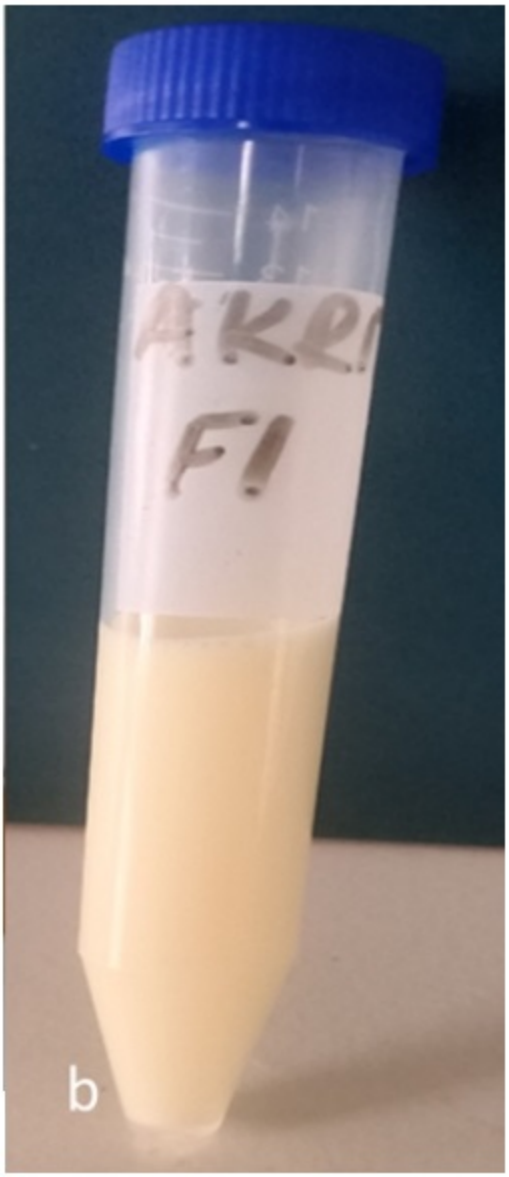

Figure 11

Figure 9 BM seed oil-loaded EVs

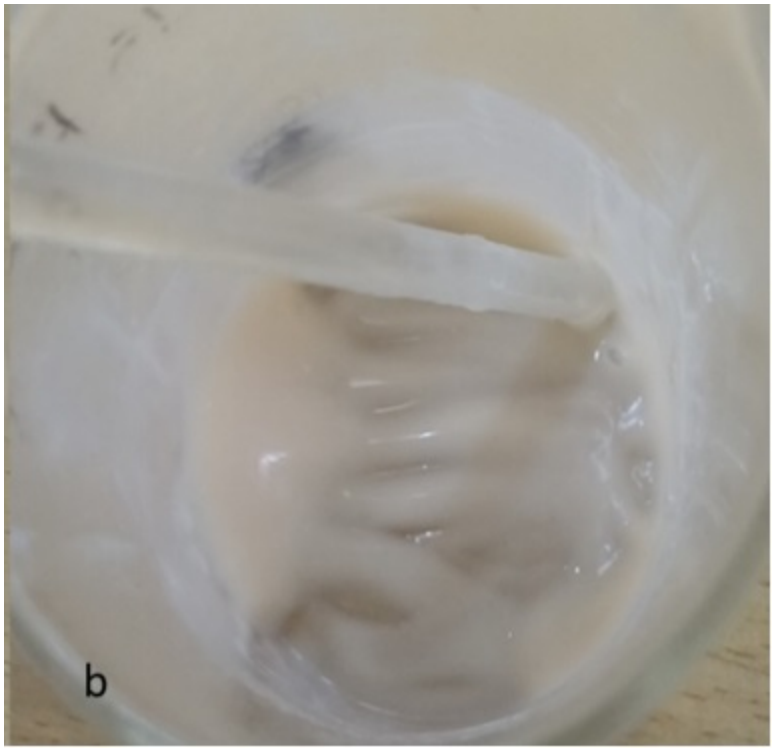

Figure 12

Figure 10 BM seed oil-loaded ethanolic vesicular hydrogel

Intensity Distribution S/N :

User	: Common	Group	:	Repetition	: 1/1
Date	: 4/2/2012	File Name	: Fourteen BBD		
Time	: 05:24:48	Sample Information	:		
SOP Name	: SOP(New)			Security	: No Security

Version 3.73 / 2.30

Intensity Distribution

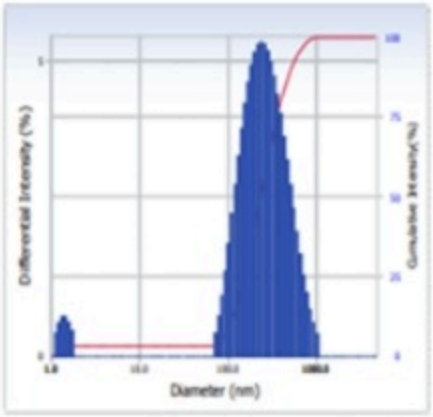

ACF

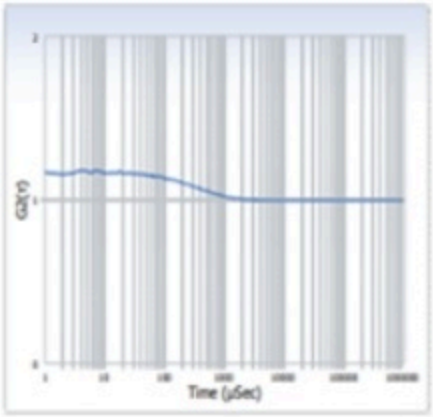

Distribution Results (Contin)

Peak	Diameter (nm)	Std. Dev.
1	1.4	0.2
2	311.1	186.4
3	0.0	0.0
4	0.0	0.0
5	0.0	0.0

Cumulants Results

Diameter	(d)	: 249.0	(nm)
Polydispersity Index	(P.I.)	: 0.301	
Diffusion Const.	(D)	: 1.993e-008	(cm^2/sec)

Measurement Condition

Temperature	: 25.0	(℃)
Diluent Name	: N W	

Figure 13

Figure 11 Particle size and PDI values of BM seed oil-loaded EVs

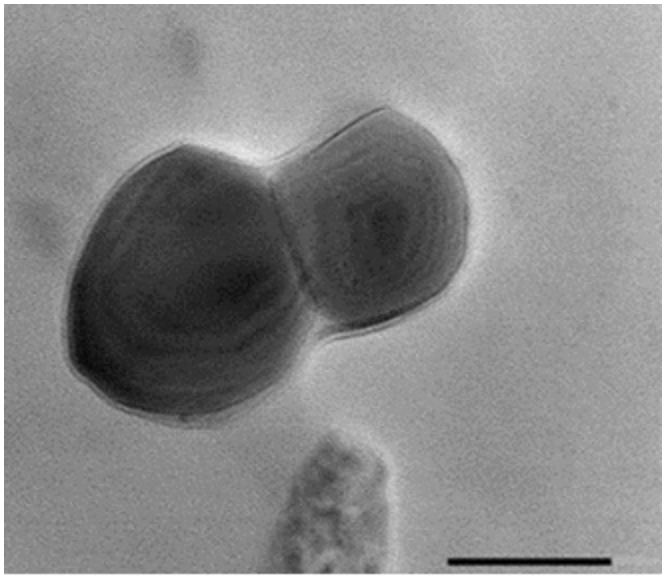

Figure 14

Figure 12 HRTEM of BM seed oil-loaded EVs

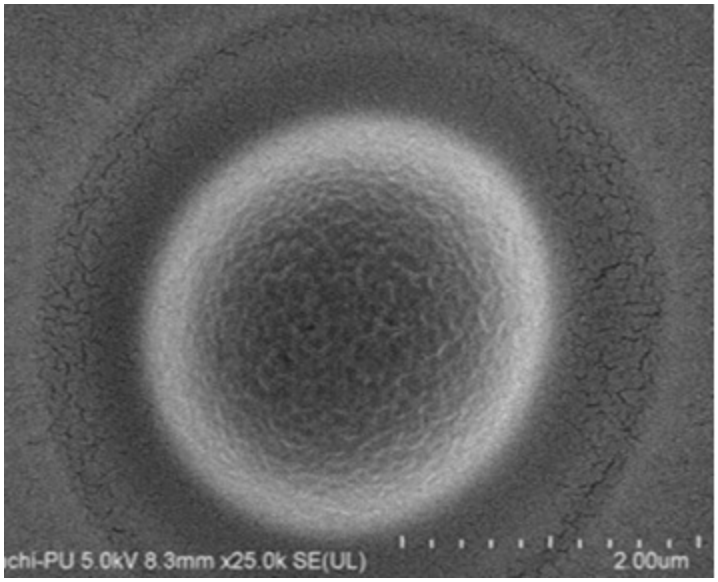

Figure 15

Figure 13 FESEM of BM seed oil-loaded EVs

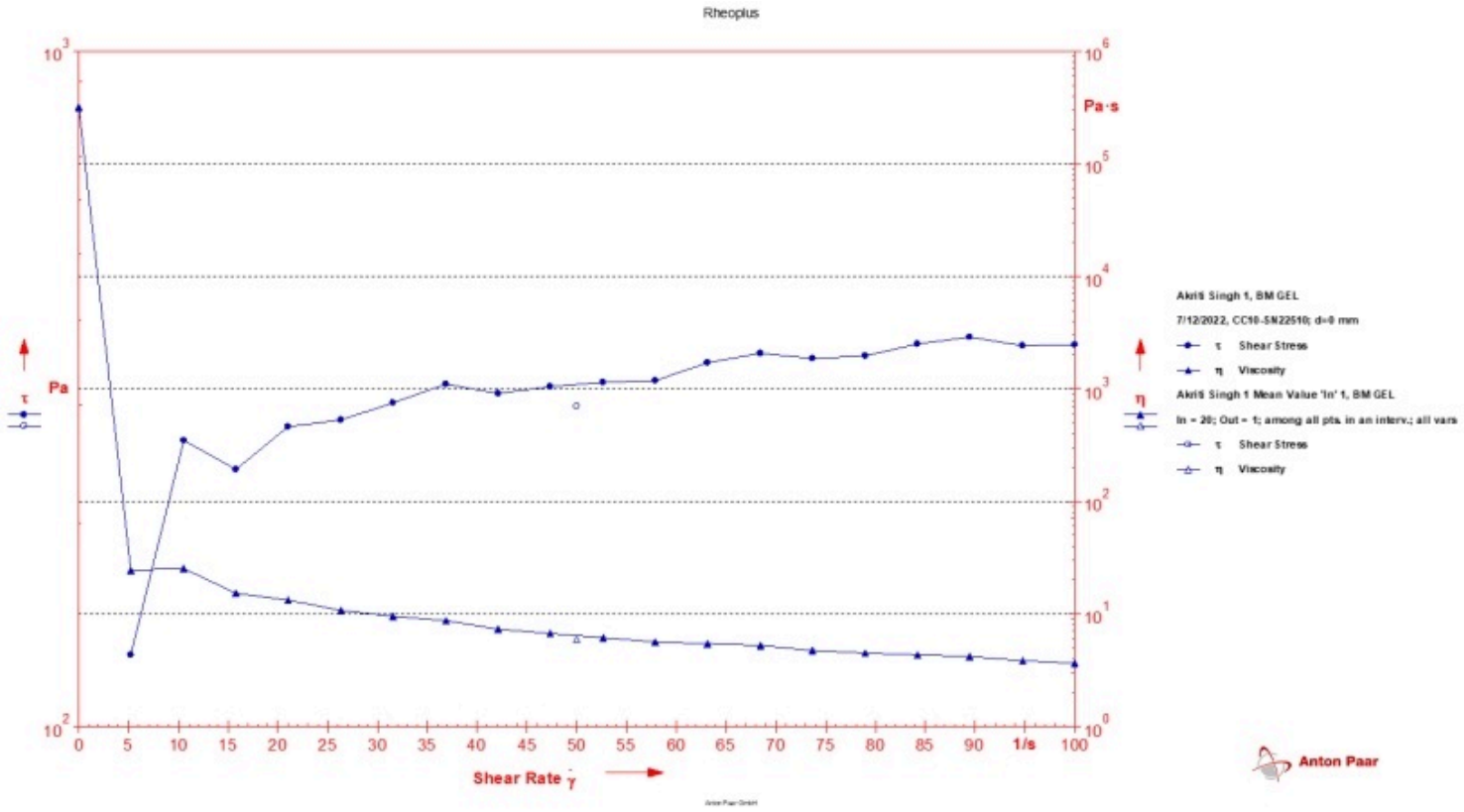

Figure 16

Figure 14 Flow curves of BM seed oil-loaded ethanolic vesicular hydrogel

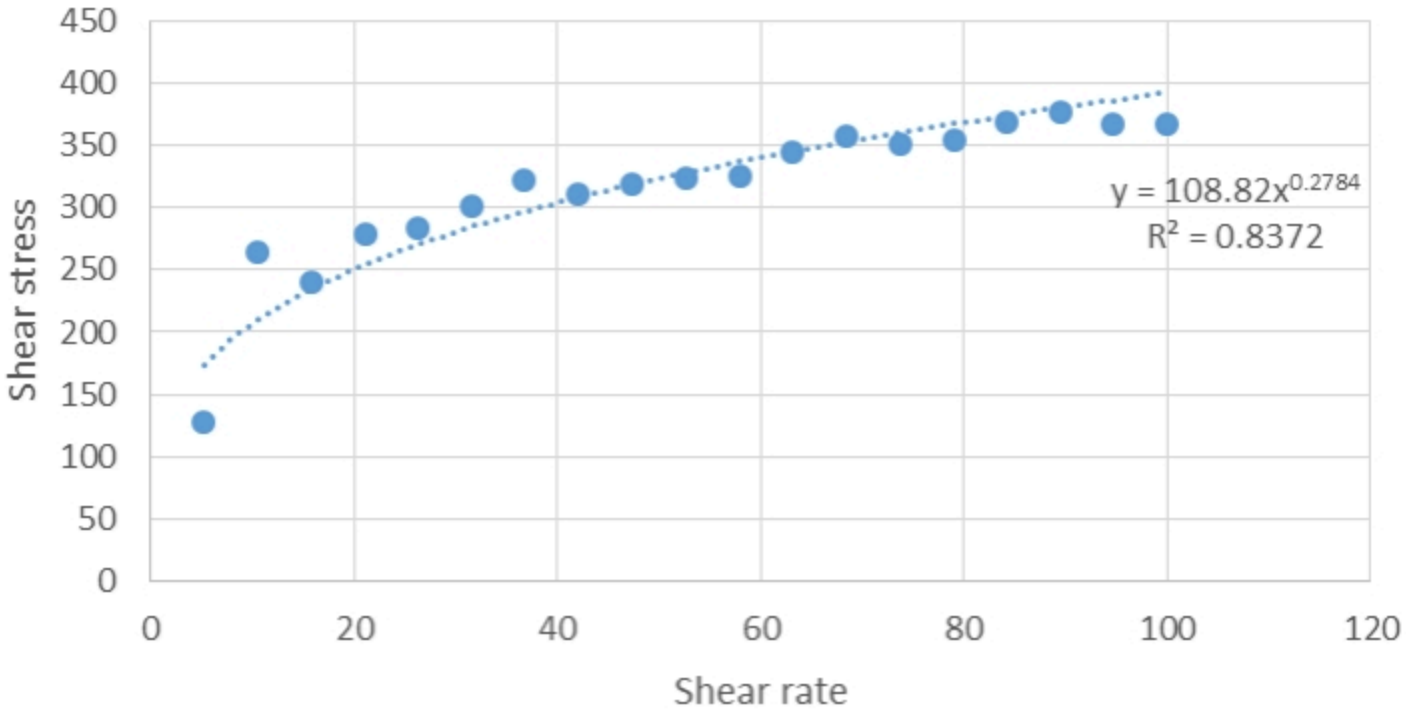

Figure 17

Figure 15 Representation of shear stress (τ) vs shear rate (γ) for BM seed oil-loaded ethanolic vesicular hydrogel

Figure 18

Figure 16 MIC of BM seed oil, BM seed oil-loaded EVs and ethanolic vesicular hydrogel

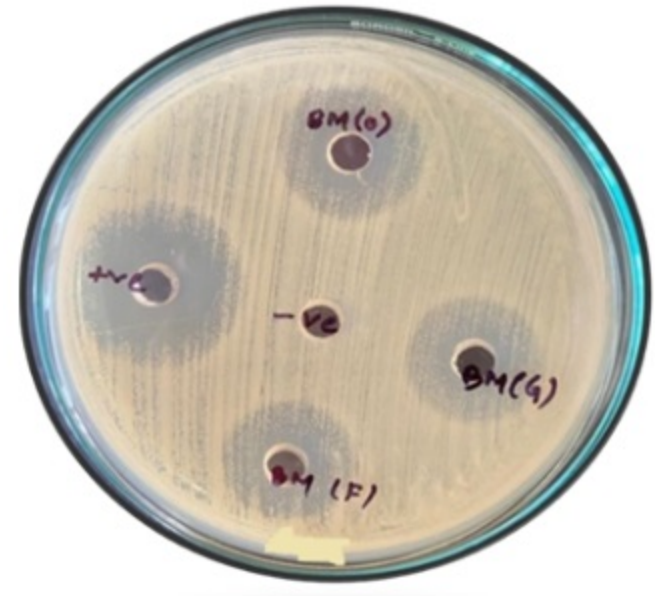

Figure 19

Figure 17 Zone of inhibition of BM seed oil, BM seed oil-loaded EVs, ethanolic vesicular hydrogel, positive control and negative control

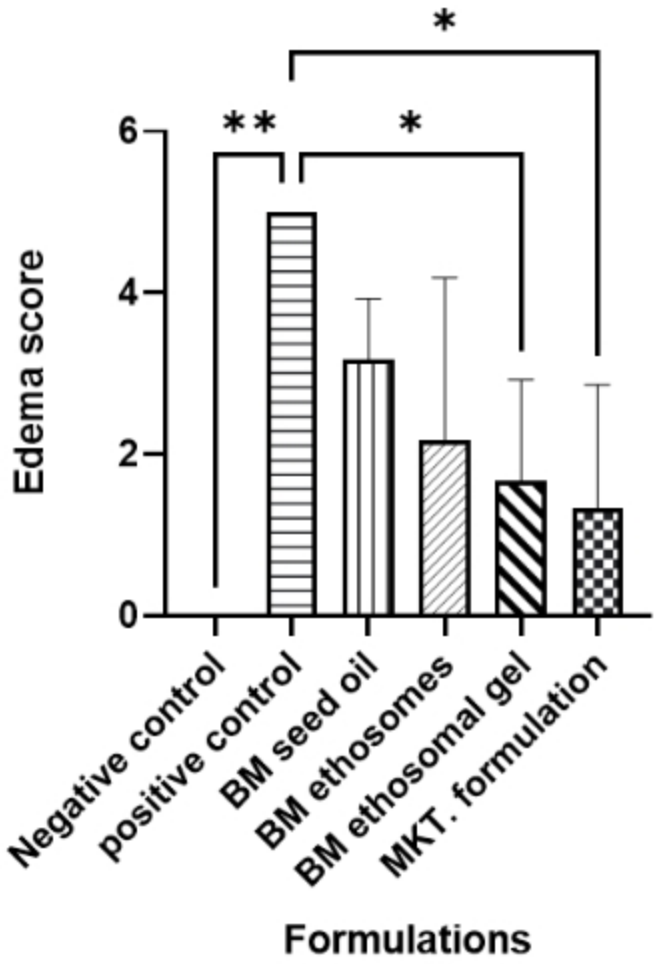

Figure 20

Figure 18 Inflammation scores for vaginal candidiasis mice model treated with various BM seed oil-loaded formulations

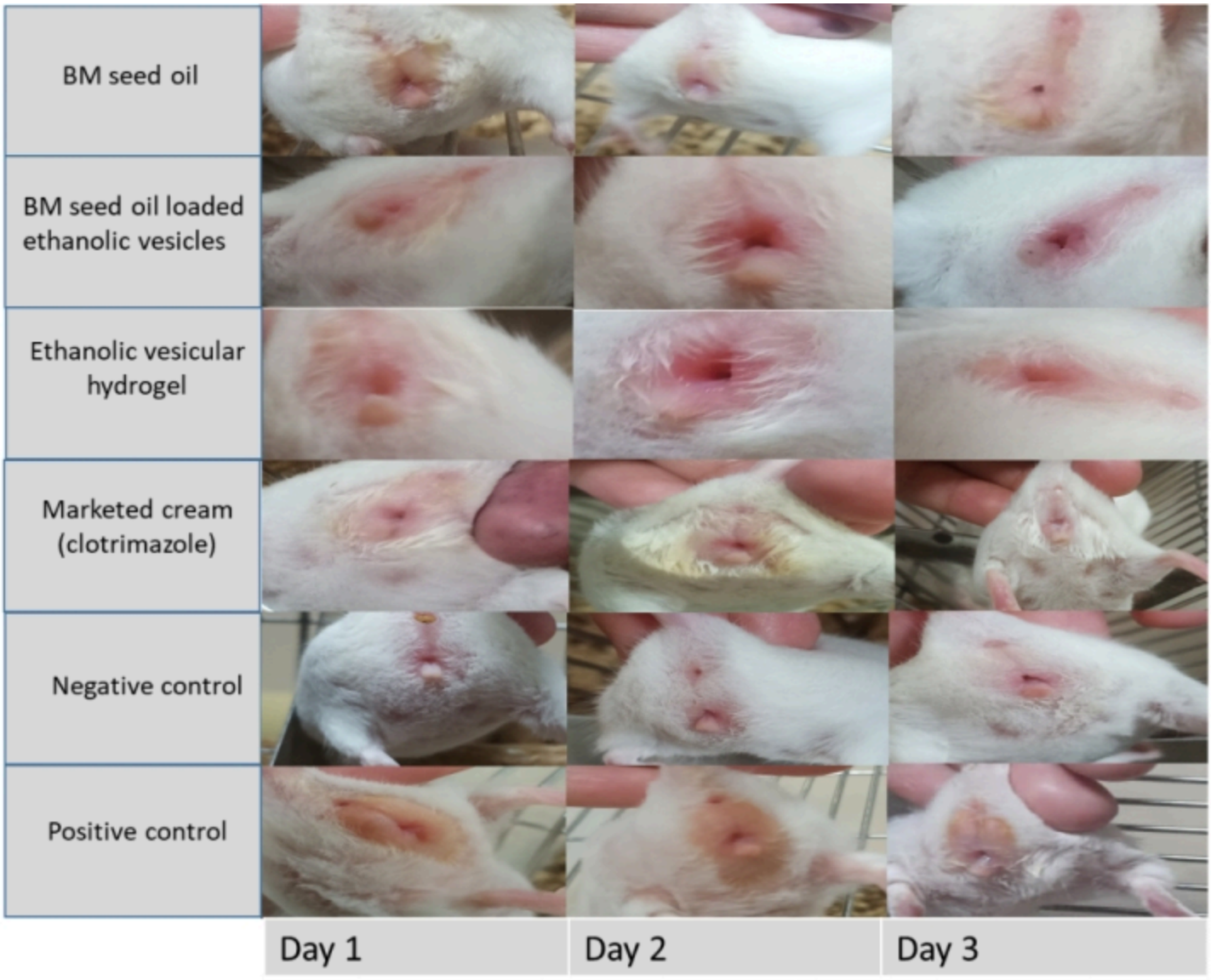

Figure 21

Figure 19 *In vivo* antifungal study of BM seed oil, BM seed oil-loaded EVs, ethanolic vesicular hydrogel, marketed cream (clotrimazole), negative control and positive control.

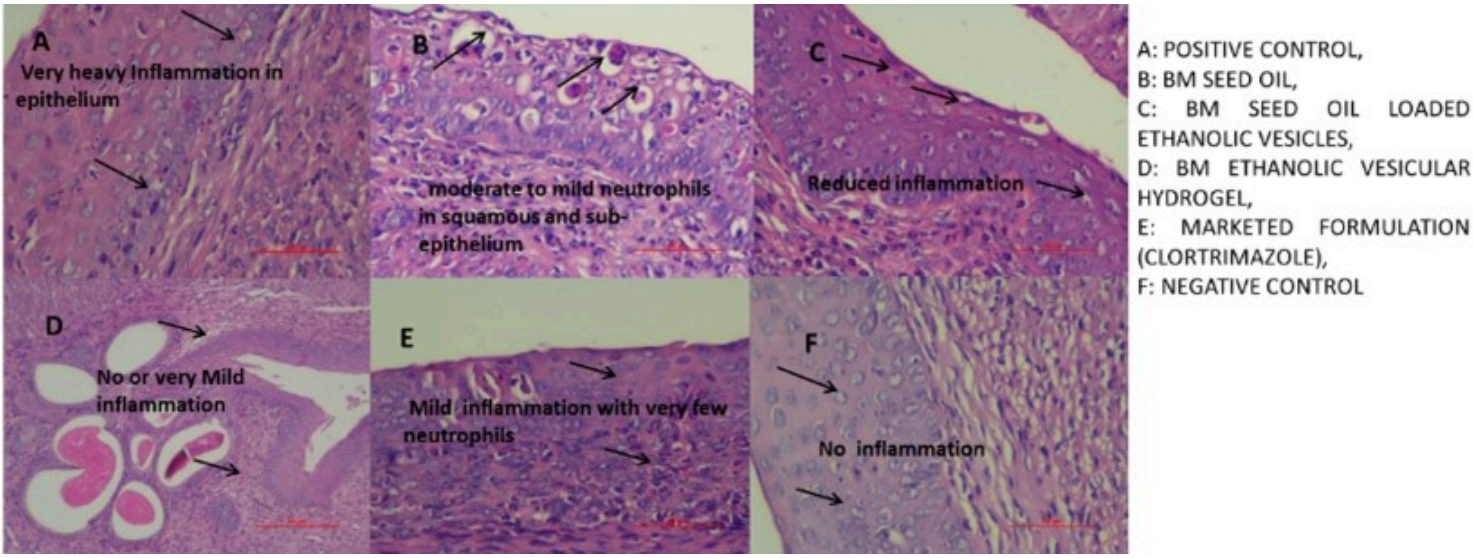

Figure 22

Figure 20 Histopathology analysis of a) Positive control, b) BM seed oil, c) BM seed oil-loaded EVs, d) BM seed oil-loaded ethanolic vesicular hydrogel treated vaginal tissue, e) marketed formulation (clotrimazole), f) negative control.